

***N*-METHYL-6-HYDROXYQUINOLIUM: AN INVESTIGATION
INTO THE SPECTROSCOPY AND APPLICATIONS OF EXCITED-
STATE PROTON TRANSFER**

A Thesis
Presented to
The Academic Faculty

by

Michael Anthony Salvitti

In Partial Fulfillment
of the Requirements for the Degree
Master of Science in Organic Chemistry
in the
Department of Chemistry and Biochemistry

Georgia Institute of Technology
August 2008

Copyright © 2008 by Michael Anthony Salvitti

**N-METHYL-6-HYDROXYQUINOLINIUM: AN INVESTIGATION
INTO THE SPECTROSCOPY AND APPLICATIONS OF EXCITED-
STATE PROTON TRANSFER**

Approved by:

Dr. Laren M. Tolbert, Advisor
Department of Chemistry and Biochemistry
Georgia Institute of Technology

Dr. Uwe Bunz
Department of Chemistry and Biochemistry
Georgia Institute of Technology

Dr. Christine Payne
Department of Chemistry and Biochemistry
Georgia Institute of Technology

Date Approved: July 7, 2008

*Dedicated to Katherine "Grandma Kas" Salvitti and
Ralph "Grandpa Ralph" Wilson*

ACKNOWLEDGEMENTS

Isaac Newton has been credited with the phrase “If I have seen further, it is by standing on the shoulders of giants.” Although I my studies thus far have only allowed me to incrementally expand the field of scientific knowledge, there are several great scientists who have assisted me during my graduate studies.

I would first like to thank Dr. Laren Tolbert. In addition to funding my graduate studies and allowing me to work on several projects of scientific and commercial interest (one of which is detailed in this thesis), he has served as an enduring source of guidance and encouragement. Likewise, I have had the pleasure of working with Dr. Kyril Solntsev who is by far the most talented spectroscopist that I have ever met, and I owe him immensely for his time teaching me the principles and practice of fluorescence spectroscopy. Dr. Janusz Kowalik has also been a tremendous help to me; his ability to improvise in the laboratory and synthetic knowledge still bewilders me to this day.

My work would not have progressed this far if it was not for the strong support of the members of my laboratory, past and present. First, I need to thank Juan Vargas and Robert Whetsell, who are members of my entering class and have been with me through all the ups and downs of graduate school. Keep some Keystone in the fridge for me, fellas. Likewise, Anthony Baldrige, Jian Dong, E.A. Gould and Russell Vegh have given me assistance as well as lively scientific discussions. Good luck to all of you throughout the rest of your graduate school careers.

The past members of the Tolbert laboratory have been great tutors and have allowed me to “learn the ropes” of laboratory research: Dr. Christina Bauer, Dr. Loretta Crowe, Dr. Jonas Jarvholm, Dr. Yu Li and Dr. Vu Nguyen. Thank you to all.

Numerous individuals have assisted me in areas outside of my own specialties. I would like to thank Richard Lawson for help with patterning and lithography; Chris Richardson for his patience and instruction on the TRSPC; Toni Bonhivert and Grant Hendrickson for their assistance with the DLS; Matija Crne for instruction on the fluorescence microscope; Dr. Oliver Poziat for transient absorbance measurements; and Dr. Alex Popov for his data-fitting models for **NM6HQ** compounds.

I am indebted to the members of my thesis committee, who have taken valuable time out of their busy schedules to provide advice and assistance: Dr. Bunz, Dr. Henderson, Dr. Payne and Dr. Srinivasarao.

Finally, my sincerest gratitude is extended to the members of my family who have given me their unconditional love and support: My parents David and Linda Salvitti, my brother Dave, Uncle Russ and Grandma Shirl.

TABLE OF CONTENTS

	Page
ACKNOWLEDGEMENTS	iv
LIST OF TABLES	viii
LIST OF FIGURES	ix
LIST OF ABBREVIATIONS	xi
SUMMARY	xii
 <u>CHAPTER</u>	
1 AN INTRODUCTION TO PROTON TRANSFER	1
A Brief History of Proton Transfer	1
Occurrences and Applications	2
ESPT in Hydroxyarenes	4
Proton Transfer in Biaryl Systems	6
Current Trends in ESPT Research	9
2 NM6HQ: THEORETICAL CONSIDERATIONS AND SYNTHESIS	11
Quaternated Hydroxyquinolinium ESPT Theory	13
Synthesis and Characterization	16
3 SPECTROSCOPY OF NM6HQ DERIVATIVES	29
UV-Visible Spectroscopy and Discussion	31
Steady-State Fluorescence Spectroscopy	32
Fluorescence Behavior in Alcohols	34
Steady-State Profiles of Varying Anions	35
Fluorescence Lifetime Measurements	38
Behavior in Non-Basic Solvents	40

Aggregation Studies	42
Dilution Experiments	42
Dynamic Light Scattering	45
Counterion Discussion	46
4 CATIONIC POLYMERIZATION INITIATED BY ESPT	48
Background Information	48
Dimethyl-4-hydroxyphenylsulfonium hexafluoroantimonate	48
Fluorinated Phenols	49
Hydroxymethyl Phenols	50
NM6HQ: Excited-State Proton Exchange with Acetone	51
Polymerization with PAGS	54
Polymerization Experiments	57
Cyclohexene Oxide	58
Dicyclopentadiene Diepoxide	61
Bisphenol A Diglycidyl Ether	62
Discussion	62
Conclusions	65
5 NM6HQ FRONTIERS	67
NM6HQ-N(Tf)₂ : A Room Temperature Ionic Liquid	67
Ratiometric Fluorescence Sensing	68
Final Thoughts	69
REFERENCES	70

LIST OF TABLES

Table 2.1:	Counterion strengths	16
Table 3.1:	Solubilities of NM6HQ salts	30
Table 3.2:	Solvatochromism in alcohols	32
Table 3.3:	Zwitterion:cation intensities in butanol	37
Table 3.4:	Dynamic Light Scattering data	45

LIST OF FIGURES

	Page
Figure 1.1: Energetic scheme of ESPT in hydroxyarenes	4
Figure 1.2: HOMO and LUMO orbital diagrams of 2N	7
Figure 1.3: HOMO and LUMO orbital diagrams of DCN2	9
Figure 2.1: Cationic, neutral, anionic and zwitterionic forms of 6HQ	13
Figure 2.2: HOMO and LUMO orbital diagrams of NM6HQ	14
Figure 2.3: Synthetic method for the preparation of NM6HQ salts	19
Figure 2.4: ¹ H NMR spectrum of NM6HQ-Nf	27
Figure 2.5: ¹ H NMR spectrum of NM6MQ-Nf	28
Figure 3.1: Absorbance of NM6HQ in alcohols	31
Figure 3.2: Fluorescence decay pathways of NM6HQ	33
Figure 3.3: Steady-state fluorescence of NM6HQ-Nf in alcohols	34
Figure 3.4: Steady-state fluorescence of NM6HQ salts in butanol	36
Figure 3.5: Steady-state fluorescence of three salts in butanol	37
Figure 3.6: NM6HQ (Z*) decays in butanol	39
Figure 3.7: NM6HQ (C*) decays in butanol	39
Figure 3.8: Fluorescence in DMSO/ACN mixtures	41
Figure 3.9: Absorbance and SS fluorescence in DMSO	42
Figure 3.10: Absorbance and SS fluorescence dilutions in methanol	43
Figure 3.11: Beer's Law plot in MeOH	44
Figure 4.1: Dimethyl-4-hydroxyphenylsulfonium mechanism	48
Figure 4.2: Hydroxymethylphenol photoacid	50
Figure 4.3: Hydrogen-deuterium exchange in d ₆ acetone	52

Figure 4.4:	NMR studies of hydrogen-deuterium exchange	53
Figure 4.5:	Proton exchange with acetone	54
Figure 4.6:	Mechanism of onium acid generation	55
Figure 4.7:	Monomers investigated for ESPT cationic polymerization	56
Figure 4.8:	Photoinitiated polymerization of CHO	58
Figure 4.9:	CHO polymerization mechanism	59
Figure 4.10:	Polymerization of CHO by NM6HQ salts	60
Figure 4.11:	Polymerization of DCPDE by NM6HQ-Nf	62
Figure 5.1:	Behavior in basic and non-basic solvents	69

LIST OF ABBREVIATIONS

Chemical Abbreviations

PAG	Photoacid generator
2N	2-Naphthol
DCN2	5,8-Dicyano-2-naphthol
6HQ	6-Hydroxyquinoline
7HQ	7-Hydroxyquinoline
6MQ	6-Methoxyquinoline
6HQNO	6-Hydroxyquinoline- <i>N</i> -oxide
NM6HQ	N-methyl-6-hydroxyquinolinium (cation)
NM6MQ	N-methyl-6-methoxyquinolinium (cation)
Nf	Nonafluorobutanesulfonate, "Nonaflate"
Tf	Trifluoromethanesulfonate, "Triflate"
N(Tf) ₂	Bis(trifluoromethylsulfonyl) Amide
CHO	Cyclohexene oxide
DCPDE	Dicyclopentadiene diepoxide
BADGE	Bisphenol A Diglycidyl Ether
RTIL	Room-temperature ionic liquid

Equipment Abbreviations

TRSPC	Time-resolved single photon counter
DLS	Dynamic Light Scattering

Chemical Process Abbreviations

ESPT	Excited-state proton transfer
ES _i PT	Excited-state intramolecular proton transfer
PTTS	Proton transfer to solvent

SUMMARY

Excited-state proton transfer (ESPT) encompasses a region of chemistry in the realm of chemical physics, but with wide-ranging applications that can extend into all branches of science. Near-instantaneous control of acidity through the manipulation of light, rather than chemically controlling the pH lends itself to fields as diverse as synthetic organic chemistry, polymer and materials science, biology, physics and engineering.

Utilizing principles of intelligent molecular design backed by molecular modeling, several salts of the N-methyl-6-hydroxyquinolinium cation (**NM6HQ**) were investigated via spectroscopic and chemical means. The goals of these experiments were twofold: to create a compound exhibiting a large pK_a drop upon photoexcitation (ideally greater than 10 units), and to investigate the interplay between the cation and its conjugate base in the excited state.

Photoacidity via ESPT was initially investigated through spectroscopic means. Fluorescence spectroscopy confirmed that some of the salts, especially those with fluorinated sulfonyl counterions, were exhibiting exceptional proton transfer in basic solvents. Light-initiated polymerizations of acid-sensitive monomers using **NM6HQ** as an initiator were examined. The results indicate that several salts of **NM6HQ** indeed undergo a large pK_a jump upon photoexcitation.

Not surprisingly, proton transfer from **NM6HQ** depends heavily on the anion. It was initially thought that exceptionally non-nucleophilic anions would increase the

excited-state acidity of the molecule. However, bulky, weakly-coordinating anions from the traditional “super acid” families actually inhibit excited-state proton transfer.

Of the several compounds tested, *N*-methyl-6-hydroxyquinolinium nonaflate (**NM6HQ-Nf**) has been shown to exhibit the largest pK_a drop upon photoexcitation; its hydroxyl moiety has a pK_a of 7 in the ground state, yet drops to a calculated pK_a^* of approximately -7 in the excited-state, determined by spectroscopic means. However, the true pK_a^* probably lies below -8 as chemical applications of the compound show. This constitutes a pK_a jump greater than 14 orders of magnitude upon photoexcitation and registers as the largest pK_a jump reported to-date via direct proton transfer.

Experiments contained herein demonstrate that excited-state proton transfer from this molecule is capable of protonating carbonyls, thereby initiating an acid-catalyzed deuterium exchange with d_6 acetone. **NM6HQ** salts have shown to be capable of initiating cationic ring opening polymerizations in cyclical aliphatic epoxides at room temperature. Likewise, this class of compounds is the first of its kind which conclusively demonstrates polymerization by proton transfer rather than hydrogen abstraction from solvent, which is seen in traditional photoacid generators.

CHAPTER 1

AN INTRODUCTION TO EXCITED-STATE PROTON TRANSFER

A Brief History of Proton Transfer

As the simplest possible ion, the proton, and consequently proton-transfer reactions, comprise a vital part of chemistry in fields as diverse as life sciences and functional materials. The H^+ ion is the fundamental basis of acid-base chemistry.

Dating to the earliest civilizations, acids have served numerous roles in society. In addition to imparting a sour flavor to food, acetic acid was a known food preservative in Egyptian and Greek times. The Arabs of 800 A.D. succeeded in isolating hydrochloric acid in their alchemistic quest of turning lead into gold, and knowledge of acids used for etching glass and metals was fairly widespread^[1].

Proton transfer in the ground state has been studied since the earliest times of modern chemistry, dating back to late eighteenth-century studies by Lavoisier and Davy. The general principles and history of ground-state acid/base chemistry are well known and can be found in any introductory chemistry textbook^[2].

Despite the utility of acids, and their principal constituents, protons, modern manufacturing methods and experimental biology require better tools to track and control protons and their corresponding acidity instantaneously. Until the development of photoacid generators (PAGs) approximately forty years ago^[3], the management of acidity has been accomplished through one of three methods: dilution, buffering, or neutralization with a base.

The very nature of excited-state proton transfer (ESPT) allows the demands of instantaneous pH manipulation to be met through the control of photons rather than by

chemical means. This could result in more facile pH management merely by controlling the excitation source.

Evidence of ESPT was first seen by Weber in 1931^[4]. While examining the fluorescent properties of naphthols and salicylates, he noticed a shift in the emission spectra as a function of pH. At a low pH, a single emission was observed. By increasing the pH of the aqueous solution, a second band of fluorescence began to appear at a longer wavelength. Terenin later noted that dual fluorescence was a consequence of ESPT, and resulted from fluorescence from two separate species^[5].

In 1949, Förster not only showed that photoexcitation of naphthols increased their acidity by encouraging excited-state deprotonation from the hydroxyl, but he also laid the groundwork for estimating their acidity^[6]. The proposed cycle bears his name: The Förster cycle. It was later shown that 2-naphthols decrease their pK_a from 9.5 in the ground state to $pK_a^* 2.5$ in the excited state^[7].

Since these early developments, new theories and analytical techniques have arisen to study the dynamic process of excited-state proton transfer. The development of ultrafast lasers has allowed the study of ESPT on the picosecond time range, and has labeled it as one of the fastest known chemical processes^[8]. Likewise, molecular orbital theory has provided insight into the excited-state electron rearrangements which allow for the fine-tuning of molecular properties to specific applications^[9].

Occurrences and Applications

Acid generation initiated through irradiation is a relatively new phenomenon, dating back to the 1960s, yet only coming into prominence within the past few decades.

Photoacid generators produce acid upon irradiation, and have been used in industry for decades, often in the form of bi- and tri- aryl ammonium, diazonium, iodonium, sulfonium or phosphonium onium salts with weakly-coordinating counterions^[10]. Cationic photoinitiated polymerizations make possible numerous applications, especially in the microelectronics industry. Photoacid generators act as photoinitiators, can be used to for catalytic depolymerization and to remove blocking groups on functionalized polymers. These processes generate latent acid residues, which may be present in the final product unless proper precautions are taken, and could impart undesirable properties into the finished product.

Increasing the pH of a solution through proton transfer rather than the dissociative hydrogen-abstraction that onium salts undergo has advantages. Ideally, excited-state proton transfer reactions dissociate protons only during a photoexcitation event, and return to ground-state pK_a when the excitation source is removed. The result is better control of the reaction at hand, whether it is a catalytic acidification or a cationic polymerization.

In the chemical realm, ESPT can be utilized for several practical purposes; it may be capable of initiating catalytic reactions and has been shown to selectively deprotect functional groups in organic synthesis^[11].

Biologists and biochemists embrace transient control of pH. For example, pH jump experiments serve as viable probes for manipulating protein folding in biological systems^[12].

Materials chemists are beginning to incorporate intramolecular excited-state proton transfer (ES_iPT) into polymers^[13], allowing new materials and even sunscreens to

dissipate degradative UV light as heat through an energy-wasting proton transfer event^[14].

ESPT in Hydroxyarenes

Since the inception of ESPT, it has been demonstrated in ammonium biaryl systems^[8] in addition to hydroxyarenes. For the sake of discussion, the following rules apply to hydroxyarenes, which were the compounds investigated in this thesis.

In the presence of an environment capable of accepting a proton, the thermodynamic cycle shown in **Figure 1.1** holds true.

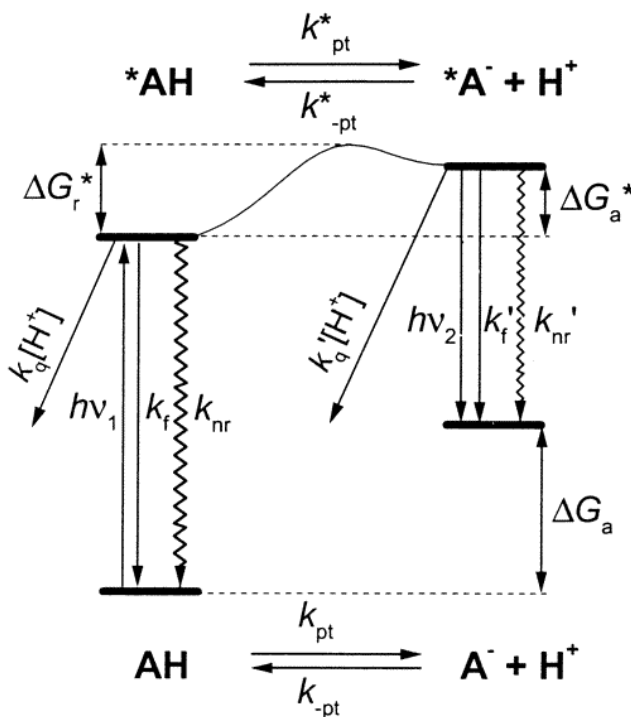


Figure 1.1 Energetic scheme of ESPT in hydroxyarenes.

In **Figure 1.1**, k_{pt}^* and k_{-pt}^* are the rates of proton dissociation and recombination in the ground and excited states, respectively, k_f and k_f' are the fluorescence decay rates

for the neutral (*AH) and anionic (*A⁻) species, respectively, k_{nr} and k_{nr}' denote the rate constants for non-radiative decay from the neutral and anionic species respectively, k_q is the constant of proton quenching, and ΔG and ΔG^* denote the entropic changes in the ground and excited states.

Utilizing this scheme first proposed by Förster, it is possible to estimate changes in acidity, based on the fluorescence spectral shift of the protonated and deprotonated molecule, assuming that the compound being investigated fluoresces in both its neutral and anionic state.

Applying general thermodynamic principles to **Figure 1.1**, it is possible to derive **Equation 1.1**:

$$\Delta H^* - \Delta H = N_A h(\nu_{RO^-} - \nu_{ROH}) \quad (1.1)$$

Assuming that the difference in enthalpy between the excited state and the ground state approximates the excited state and ground state free energy of proton transfer, it is possible to conclude that:

$$\Delta G^* = 2.3 RT pK_a^* \quad (1.2)$$

and likewise:

$$pK_a^* = pK_a + \Delta E_{0,0}/2.3RT \quad (1.3)$$

This can be simplified further to:

$$pK_a^* = pK_a - (h\nu_1 - h\nu_2)/2.3RT \quad (1.4)$$

This relationship, **Equation 1.4**, is known as the Förster equation. It is best to treat this equation as an approximation because neither changes in the surrounding solvent shell nor changes in the photoacid's geometry upon excitation are factored into the calculation. Nevertheless, it serves as an estimate of excited-state photoacidity which can be derived from spectroscopic measurements.

Proton Transfer in Biaryl Systems

The molecule 2-naphthol (**2N**) has been a proven workhorse of proton transfer physics since the phenomenon itself was discovered^[6]. The hydroxyl moiety of **2N** is capable of transferring a proton readily to basic proton accepting solvents (water, DMSO, amines, alcohols) as well as exhibiting fluorescence from both its neutral and anionic state. Upon excitation at its lowest energy transition, two bands of fluorescence are seen in either proton-accepting solvents, or under basic conditions in inert solvents. The longer wavelength emission corresponds to fluorescence of the anion, and the shorter wavelength emission corresponds to fluorescence from the neutral molecule. These emissions are solvent dependent. Hence in solvents that exhibit ESPT, the longer wavelength emission is favored; in solvents that do not accept a proton, only the shorter wavelength emission from the neutral compound is observed.

Though **2N** serves as a good model for excited state proton transfer reactions, its pK_a^* reaches only 2.5^[6]; it only becomes a mild acid in its excited state. Many applications require a higher acidity. The 2-naphtholate counterion of the proton has comparatively high nucleophilicity and competes intensely for the proton thus limiting excited-state acidity. Hence, a model of ESPT was devised to model the excited state and give a rough estimate of excited state photoacidity^[9].

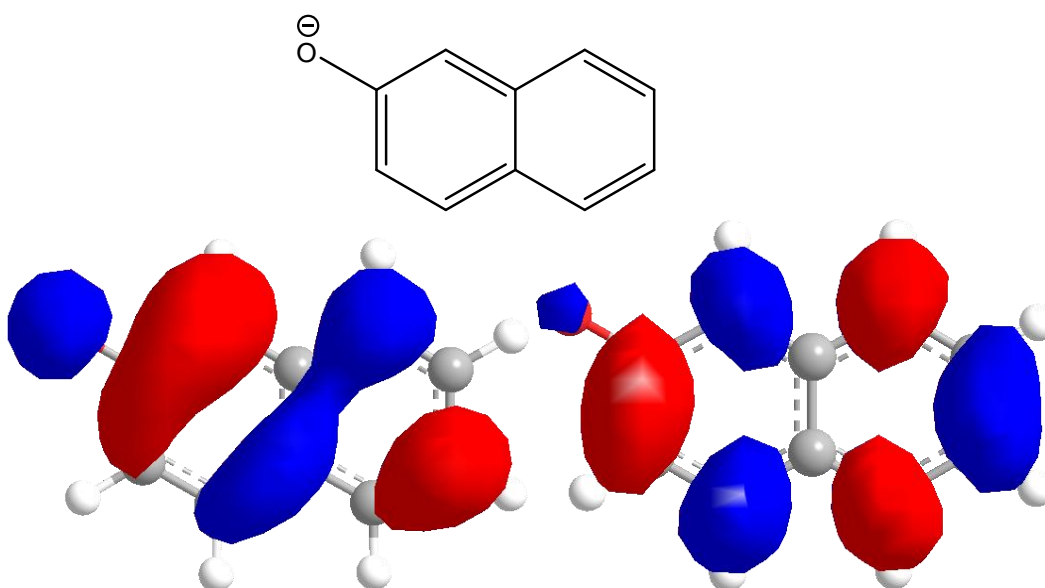


Figure 1.2 HOMO and LUMO orbital diagrams of **2N**

A simplified method of predicting photoacidity lies in calculating the redistribution of electrons between the highest occupied molecular orbital (HOMO) and the lowest unoccupied molecular orbital (LUMO) for the phenolate of the compound in question. In hydroxyarene photoacids, absorption of a photon enables a HOMO→LUMO transition. Electronic distribution shifts away from the hydroxyl group and towards the ring, delocalizing the electrons throughout the molecule. Redistribution throughout the conjugated π -system pulls electron density away from the O-H bond allowing for

dissociation of the proton and the phenolate. This phenomenon results in a large pK_a drop upon photoexcitation. **Figure 1.2** demonstrates this delocalization. Electron density surrounding the phenolate decreases significantly upon photoexcitation.

In earlier work, it was found that by moving electron-withdrawing groups (EWG) to sites distal from the proton-donating hydroxyl moiety, photoacidity could be increased^[15]. It was found that EWG placed at strategic sites that are susceptible to receiving electron localization in the excited state on the distal aromatic ring increased the photoacidity. Specifically, substitutions at the 5- and the 8- positions of 2-naphthol with electron-withdrawing nitriles led to the development of 5,8 dicyano 2-naphthol (**DCN2**), which enables a calculated pK_a^* of -4.5 ^[9]. This molecule is displayed in **Figure 1.3**. Until recently this compound exhibited the largest photoinitiated pK_a jump to date and has served as a widely-used probe for numerous pH jump experiments^[16, 17].

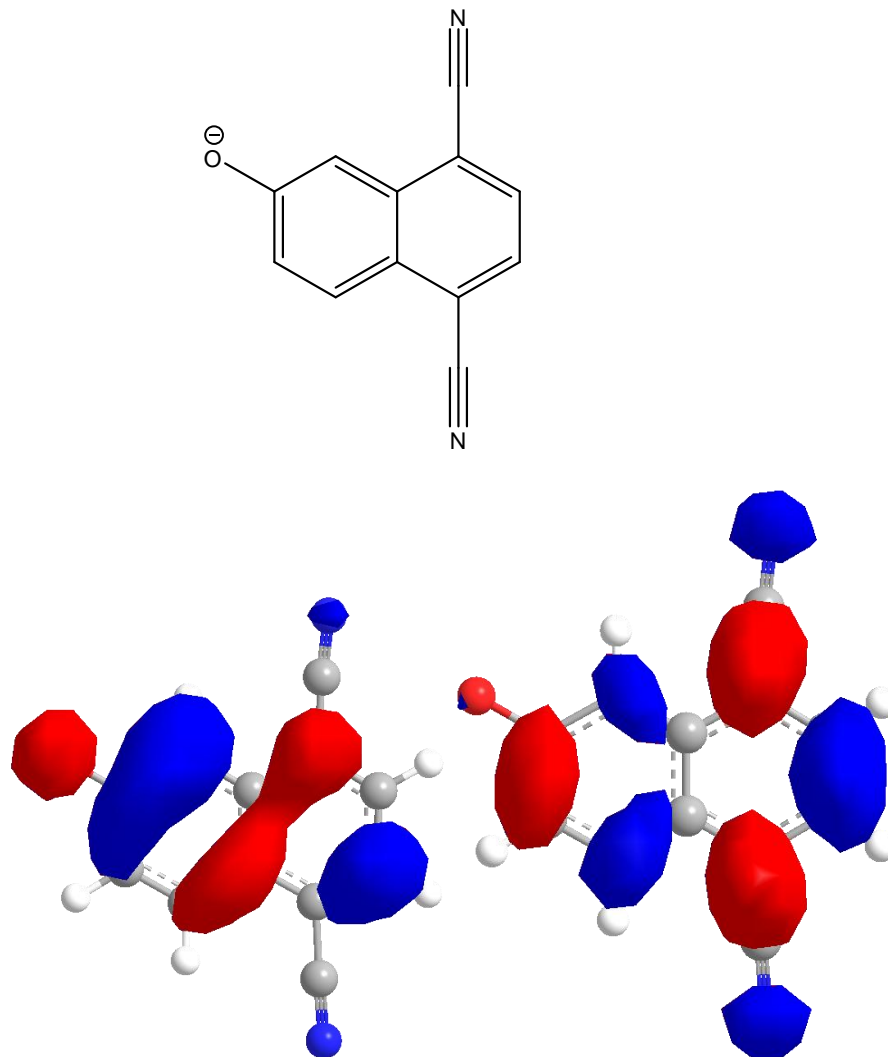


Figure 1.3 HOMO and LUMO orbital diagrams of **DCN2**.

Current Trends in ESPT Research

Despite **DCN2** acting as a powerful transient “super photo acid” with a drop of approximately 13 pKa units^[15], less research has taken place utilizing biaryl molecules with even stronger Hammett substituents than the success of **DCN2** warranted.

Utilizing the groundwork laid in prior research, this thesis aims to examine various salts of *N*-methyl-6-hydroxyquinolinium (**NM6HQ**) which have been overlooked with regards to ESPT.

Examining the effects on an organic salt complicates the matter; an additional component of the system must be considered. Most compounds exhibiting ESPT studied to date are neutral organic molecules. However, this nuance allows reconciliation of the counterion strength with excited-state acidity, and has surprisingly not been specifically examined in chemical literature.

Successful investigation into this class of compounds will open the door for further study in the following fields of chemistry: ultrafast proton transfer processes, biological pH-jump experimentation, dual-emission fluorophores, and better precision and control of reactions through transient acid generation processes.

CHAPTER 2

NM6HQ: THEORETICAL CONSIDERATIONS AND SYNTHESIS

Increasing the excited state acidity in a compound can roughly be correlated with enhanced intramolecular charge transfer to the distal ring in bicyclic hydroxyaromatic systems upon excitation. Electron donors and acceptors both respectively become stronger donors and acceptors in the excited state^[18]. Thus, it is possible to design and tailor aromatic systems and control excited state acidity by placing substituents along the aromatic rings.

Experiments and theory have demonstrated that the 5- and 8- positions of a 2-naphthol are the sites most susceptible to electron reception in the excited state, and consequently it makes sense to place stronger electron-withdrawing substituents at these positions^[18].

To this end, hydroxyquinolines comprise a logical research extension to naphthol systems, in that they are aromatic and isoelectronic to naphthols. Specifically, quinolines which are hydroxyl- substituted at the 6- and 7- positions should emulate naphthols with substituents at the 5- and the 8- positions, respectively.

Current research in the field of hydroxyquinolines has centered on 7-hydroxyquinoline and 8-hydroxyquinoline, with good reason; since both compounds exhibit a small distance between the proton donor and acceptor, proton transfer can be observed from the hydroxyl to the nitrogen, and only simple molecular modeling protocols are required to reduce experimental results to a model. Additionally, they can act as fluorogenic metal chelators due to the proximity of the donor and acceptor^[19].

The 6-hydroxyquinoline (**6HQ**) molecule has gone largely unstudied due to the large distance between the donor and the accepting moiety compared to 7- and 8-hydroxyquinolines. Many studies have looked at these compounds with regards to the solvent-assisted proton transfer from hydroxyl-to-nitrogen.

The few studies undertaken on this compound show that excited-state deprotonation occurs at the hydroxyl group even in 10M perchloric acid solutions^[20]. It is indeed a powerful proton donor in the excited state. Incidentally, the nitrogen moiety acts as a strong photo base upon excitation.

6HQ serves a role of an academic curiosity; it is a bi-functional light-induced donor/acceptor exhibiting a double proton transfer (proton transfer from hydroxyl to solvent followed by proton transfer from solvent to nitrogen), in addition to showing enhanced photobasicity on the heterocyclic nitrogen during photoexcitation. The nitrogen is capable of accepting a proton even in 12M NaOH^[20]. **Figure 2.1** shows four tautomers of **6HQ** present under different solvent conditions.

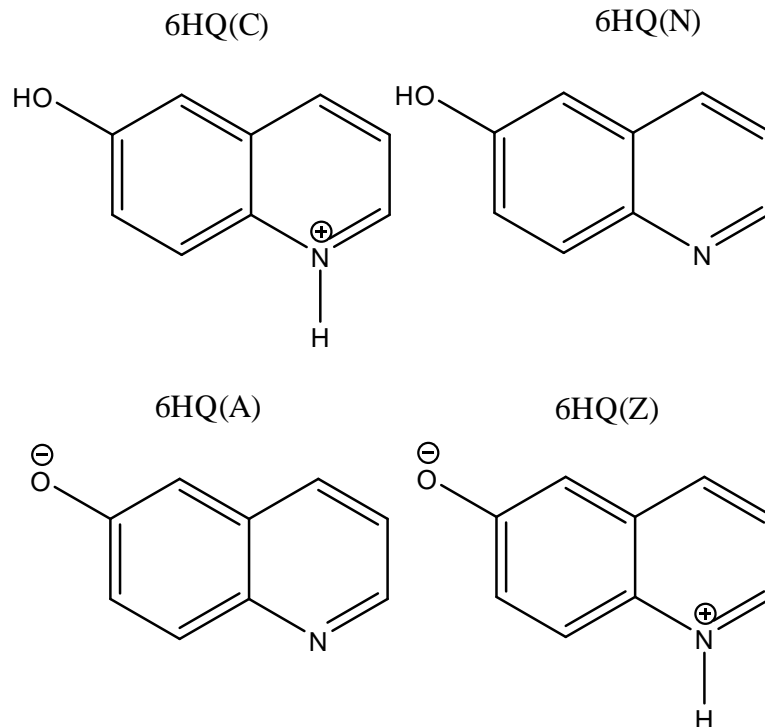


Figure 2.1 Cationic, neutral, anionic and zwitterionic forms of **6HQ**.

Quaternated Hydroxyquinolinium ESPT Theory

One serious drawback to utilizing **6HQ** in an acid-generating capacity, and thus for applications requiring acid generation, is the photobasicity of its heterocyclic nitrogen. A straightforward method of preventing excited state proton recombination at this site is to “block” the basic nitrogen lone pair. Modification of the molecule in this manner generates a quaternary ammonium salt, yet the molecule retains its aromaticity, facilitating electron transfer in the molecule after the photoinduced deprotonation. This method contains the added bonus of creating an extremely strong Hammett parameter effect in the molecule.

This phenomenon was previously investigated by oxidizing the aromatic nitrogen, thereby creating 6-hydroxyquinoline-*N*-oxide (**6HQNO**)^[21]. As expected, the excited-

state acidity increased measurably, but side reactions occurred. Photodeoxygenation and 1,2 oxygen migration of the **6HQNO** may limit use in applications such as cationic initiation, as unnecessary side products may arise depending on substrates' susceptibilities to oxidation.

Another method of preventing proton back-transfer is by alkylation of the nitrogen. This approach was undertaken for **6HQ** and **7HQ**, and the results were as expected; after methylation of the heterocyclic nitrogen with methyl iodide, both quinolinium compounds exhibited efficient proton transfer to solvent^[22]. However, this came at a cost of lowering the ground state pK_a by 2 units^[20] from pK_a 9 (**6HQ**) to pK_a 7 (**NM6HQ-I**). The effect of reducing excited-state electron density on the phenolate is seen in **Figure 2.2**. This is the method employed in the following research.

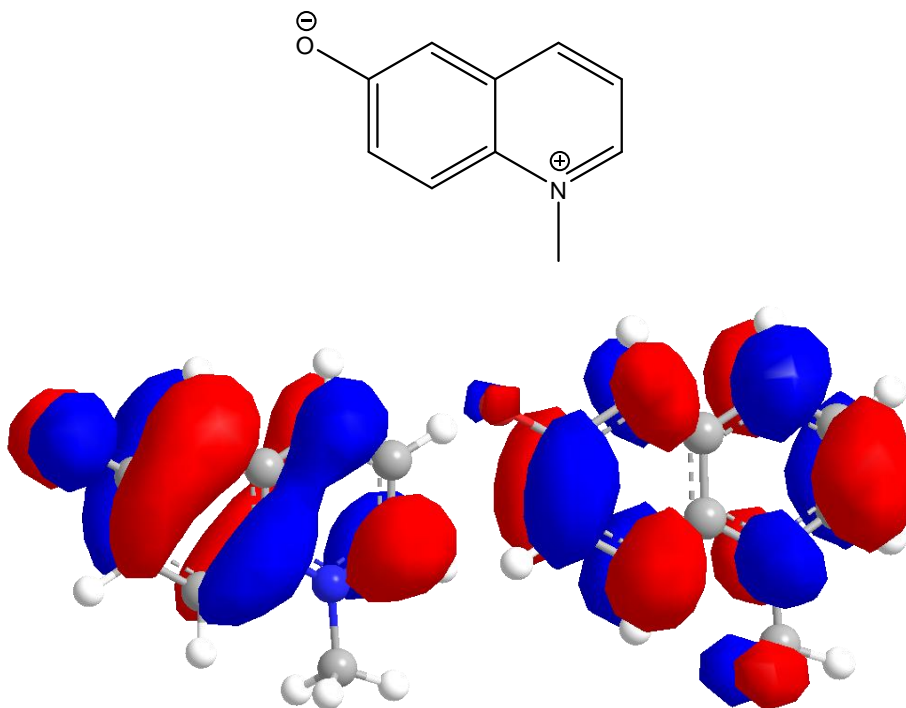


Figure 2.2 HOMO and LUMO orbital diagrams of **NM6HQ**.

Surprisingly, research-to-date has not examined anionic effects in ESPT. Hydroxyquinolinium compounds are a logical compound to undertake these studies due their large pK_a jump and fluorescent photoproducts. Only the iodide and perchlorate counterions for **NM6HQ** have been synthesized^[20, 22, 23], and no systematic investigations in the entire field of ESPT have attempted to reconcile counterion nucleophilicity with excited-state acidity. Without such investigations, it is impossible how to determine exactly how acidic these molecules can become upon excitation.

Counterion substitutions in aromatic organic salts not exhibiting proton transfer or photo acid generation generally only differ in physical properties and in the rate of photobleaching^[24, 25] without a significant change in the absorbance or fluorescence wavelengths and lifetimes, assuming that the anion is not photoactive. It remains to be seen whether this is the case for molecules which exhibit ESPT.

Many questions remain unanswered. Does the anion act as an excited-state proton acceptor in a non-accepting solvent? Is the anion capable of electron donation to the quinolinium, resulting in altered effects? These queries form the basis of research presented in this chapter.

Indeed, the conjugate acids of the iodide and perchlorate are effectively “super acids” (i.e. stronger than H_2SO_4 by definition). It is logical to assume more weakly coordinating bases could lead to stronger excited-state photoacids.

Table 2.1 Counterion strengths based on gas phase N-H bond ammonia IR vibrations. Longer frequencies correlate with weaker anionic strength^[26].

Anion	ν N-H	$\Delta\nu$ N-H
B(C₆F₅)₄⁻	3233	30
CMeB₁₁F₁₁⁻	3219	40
PF₆⁻	3191	72
SbF₆⁻	3175	88
BF₄⁻	3133	130
C₅(CN)₅⁻	3097	166
N(SO₂CF₃)₂⁻	3086	177
ClO₄⁻	3050	214
FSO₃⁻	3040	310
CF₃SO₃⁻	3030	324

As **Table 2.1** shows, several options exist for anions less nucleophilic than iodide and perchlorate based upon gas phase acidities measuring N-H bond stretching in ammonia^[26]. The molecules synthesized in this section were selected based on two criteria: they have weakly coordinating counterion strength and they are readily commercially available.

Synthesis and Characterization

General synthetic procedure:

6-Hydroxyquinoline (98%), 6-methoxyquinoline (98%), methyl iodide and the silver salts of hexafluoroantimonate, triflate, hexafluorophosphate, tetrafluoroborate and bis(trifluoromethylsulfonyl) amide were purchased from Acros and used without further purification.

Methyl trifluoromethanesulfonate (99%) and methyl nonafluorobutanesulfonate (99%) were purchased from Synquest Laboratories and used without further purification.

N-methyl 6-hydroxyquinolinium iodide, bromide, trifluoromethanesulfonate (triflate) and nonafluorobutanesulfonate (nonaflate) were synthesized using a procedure modified from the literature^[22]. This new procedure carried out the reaction in acetone instead of toluene, favoring precipitation of the final products from solution while keeping unreacted reagents soluble. Reactions were carried out in a high-pressure vial rather than a round-bottom flask to prevent the escape of volatile methylating reagents. These improvements allowed for several samples to be synthesized simultaneously in a heating block. A faster reaction time and an easier product work-up came at the expense of 5-10% sacrifice in yield.

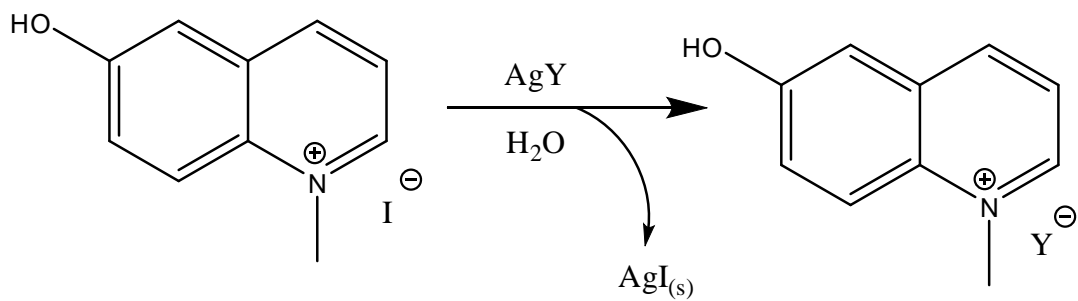
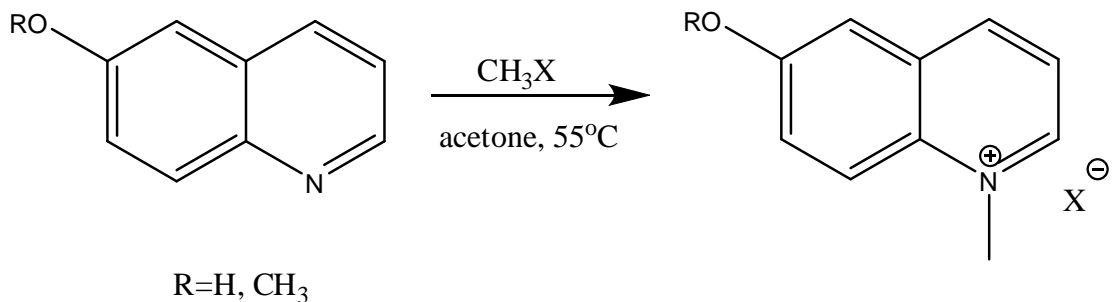
One molar equivalent of **6HQ** and 1.1 molar equivalents of the appropriate methylating reagent were dissolved in dry acetone. The reaction was heated at reflux for 4 h under pressure to prevent the escape of volatiles. After the reaction was complete the products were precipitated with diethyl ether and filtered. The products were hot-filtered from activated carbon in ethanol, and recrystallized twice in an ethanol-ether solvent mixture.

N-methyl-6-methoxyquinolinium (**NM6MQ**) iodide and nonaflate were synthesized under the same conditions as the **NM6HQ** salts described above from 6-methoxyquinoline (**6MQ**).

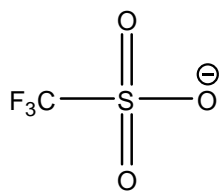
Anion metathesis was performed in water with silver salts containing the desired counterion. Silver salts were chosen because metathesis with sodium and potassium salts lead to no observable exchange; KBr and NaBr have approximately the same solubility in water, methanol, acetone as does **NM6HQ-Br**, rendering the exchange difficult in these and other common organic solvents.

Tetrafluoroborate, hexafluorophosphate, hexafluoroantimonate, bis(trifluoromethylsulfonyl) amide, and triflate containing silver salts (1.1 eq) were stirred with one molar equivalent of **NM6HQ** iodide in deionized water. Silver iodide precipitated immediately from solution. The mother liquor was recovered after filtration of the insoluble AgI, and the water was removed with a rotary evaporator. After dissolving the precipitate in ethanol, the salts were hot-filtered over activated carbon and filtered to remove the remaining traces of silver. Recrystallization was from ethanol-ether.

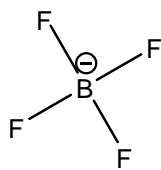
All samples were dried for 24 h at 110°C in vacuo over P₂O₅.



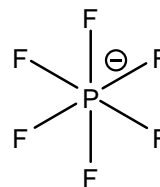
Anions investigated:



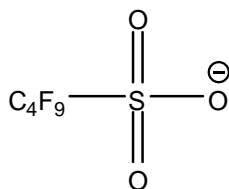
Triflate



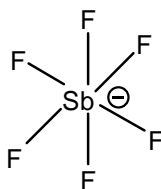
Tetrafluoroborate



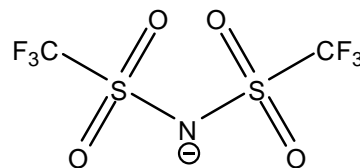
Hexafluorophosphate



Nonaflate



Hexafluoroantimonate



Bis(triflyl) Amide

Figure 2.3 Synthetic method for the preparation of **NM6HQ** salts.

Nuclear magnetic resonance spectra were recorded on a Varian Gemini 300 MHz spectrometer. Chemical shifts are reported in delta (δ) units, parts per million (ppm), relative to the chemical shift of d_5 acetone (2.05 ppm). Splitting patterns are abbreviated as follows: s, singlet; d, doublet; t, triplet; q, quartet; m, multiplet; br, broad.

Mass spectra were taken by the Georgia Institute of Technology Bioanalytical Mass Spectrometry Facility. Samples submitted for mass spectrometry were dissolved in acetone and were the same samples used for NMR. Electron Ionization (EI) spectra were collected at 400 K.

Melting points were taken with an Electrothermal capillary melting point apparatus and are reported uncorrected.

***N*-Methyl-6-Hydroxyquinolinium Iodide (NM6HQ-I).** 6-Hydroxyquinoline (0.302 g, 2.09 mmol) was added to dry acetone (4 mL) and sonicated until completely dissolved. Methyl iodide (0.368 g, 2.59 mmol) was added to the solution, and the vial was capped. The 5 mL high-pressure vial was heated at 80 °C for four hours, after which the contents of the vial were poured into 20 mL of diethyl ether. The resulting solid was filtered and rinsed with cold Et₂O. After a hot-filtration with 10 mg activated charcoal in ethanol, the product was again precipitated with Et₂O and recrystallized from an ethanol-ether mixture. After drying at 110 °C in vacuo over P₂O₅, the desired product (0.366 g, 1.28 mmol, 61.1% yield) was recovered as shiny yellow-light green crystals, mp 224-226 °C. ¹H NMR (300 MHz, Acetone) δ 10.09 (s, 1H), 9.34 (d, J = 5.0, 1H), 9.10 (d, J = 8.5, 1H), 8.54 (d, J = 9.5, 1H), 8.11 (dd, J = 5.7, 8.5, 1H), 7.92 (dd, J = 2.8, 9.6, 1H), 7.75 (d, J =

2.7, 1H), 4.84 (s, 3H); EIMS, m/z 160.1 (M^+ , 24%), 145.1 (100%), 89.1, 63.1; MS (EI, m/z), calcd. for $C_{10}H_{10}NO$: 160.076. Found: 160.1.

***N*-Methyl-6-Hydroxyquinolinium Bromide (NM6HQ-Br).** 6-Hydroxyquinoline (0.214 g, 1.47 mmol) was added to dry acetone (4 mL) and sonicated until completely dissolved. Methyl bromide (0.195 g, 2.05 mmol) was added to the solution, and the vial was capped. The 5 mL high-pressure vial was heated at 80 °C for four hours, after which the contents of the vial were poured into 20 mL of diethyl ether. The resulting solid was filtered, and rinsed with cold Et_2O . After a hot-filtration with 10 mg activated charcoal in ethanol, the product was again precipitated with Et_2O and recrystallized from an ethanol-ether mixture. After drying at 110 °C in vacuo over P_2O_5 , the desired product (0.032 g, 0.13 mmol, 9.1% yield) was recovered as shiny white/light pink crystals, mp 245-246 °C. 1H NMR (300 MHz, Acetone) δ 10.09 (s, 1H), 9.34 (d, J = 5.0, 1H), 9.10 (d, J = 8.5, 1H), 8.54 (d, J = 9.5, 1H), 8.11 (dd, J = 5.7, 8.5, 1H), 7.92 (dd, J = 2.8, 9.6, 1H), 7.75 (d, J = 2.7, 1H), 4.84 (s, 3H). EIMS, m/z 160.1 (M^+ , 24%), 145.1 (100%), 89.1, 63.1; MS (EI, m/z), calcd. for $C_{10}H_{10}NO$: 160.076. Found: 160.1.

***N*-Methyl-6-Hydroxyquinolinium Triflate (NM6HQ-Tf).** 6-Hydroxyquinoline (0.169 g, 1.17 mmol) was added to dry acetone (4 mL) and sonicated until completely dissolved. Methyl triflate (0.247 g, 1.51 mmol) was added to the solution, and the vial was capped. The 5 mL high-pressure vial was heated at 80 °C for four hours, after which the contents of the vial were poured into 20 mL of diethyl ether. The resulting solid was filtered, and rinsed with cold Et_2O . After a hot-filtration with 10 mg activated charcoal in ethanol, the

product was again precipitated with Et₂O and recrystallized from an ethanol-ether mixture. After drying at 110 °C in vacuo over P₂O₅, the desired product (0.239 g, 0.773 mmol, 66.11% yield) was recovered as a fine white powder, mp 100-102 °C. ¹H NMR (300 MHz, Acetone) δ 10.09 (s, 1H), 9.34 (d, J = 5.0, 1H), 9.10 (d, J = 8.5, 1H), 8.54 (d, J = 9.5, 1H), 8.11 (dd, J = 5.7, 8.5, 1H), 7.92 (dd, J = 2.8, 9.6, 1H), 7.75 (d, J = 2.7, 1H), 4.84 (s, 3H). EIMS, m/z 160.1 (M⁺, 24%), 145.1 (100%), 89.1, 63.1; MS (EI, m/z), calcd. for C₁₀H₁₀NO: 160.076. Found: 160.1.

***N*-Methyl-6-Hydroxyquinolinium Nonaflate (NM6HQ-Nf).** 6-Hydroxyquinoline (0.170 g, 1.17 mmol) was added to dry acetone (4 mL) and sonicated until completely dissolved. Methyl nonaflate (0.320 g, 1.02 mmol) was added to the solution, and the vial was capped. The 5 mL high-pressure vial was heated at 80 °C for four hours, after which the contents of the vial were poured into 20 mL of diethyl ether. The resulting solid was filtered, and rinsed with cold Et₂O. After a hot-filtration with 10 mg activated charcoal in ethanol, the product was again precipitated with Et₂O and recrystallized from an ethanol-ether mixture. After drying at 110 °C in vacuo over P₂O₅, the desired product (0.127 g, 0.277 mmol, 23.7% yield) was recovered as a fine white powder, mp 125-126 °C. ¹H NMR (300 MHz, Acetone) δ 10.09 (s, 1H), 9.34 (d, J = 5.0, 1H), 9.10 (d, J = 8.5, 1H), 8.54 (d, J = 9.5, 1H), 8.11 (dd, J = 5.7, 8.5, 1H), 7.92 (dd, J = 2.8, 9.6, 1H), 7.75 (d, J = 2.7, 1H), 4.84 (s, 3H). EIMS, m/z 160.1 (M⁺, 24%), 145.1 (100%), 89.1, 63.1; EIMS, m/z 160.1 (M⁺, 24%), 145.1 (100%), 89.1, 63.1; MS (EI, m/z), calcd. for C₁₀H₁₀NO: 160.076. Found: 160.1.

***N*-Methyl-6-Methoxyquinolinium Iodide (NM6MQ-I).** 6-Methoxyquinoline (0.265 g, 1.66 mmol) was added to dry acetone (3mL) and sonicated until completely dissolved. Methyl iodide (approximately twofold excess) was added to the solution, and the vial was capped. The 5mL high-pressure vial was heated at 80°C for four hours, after which the contents of the vial were poured into 20 mL of diethyl ether. The resulting solid was filtered, and rinsed with Et₂O. After a hot-filtration with 10mg activated charcoal in ethanol, the product was again precipitated with Et₂O and recrystallized from an ethanol-ether mixture. After drying at 110°C in vacuo over P₂O₅, the desired product (0.4457 g, 1.48 mmol, 89.2% yield) was recovered as bright yellow crystals, mp 236-237 °C. ¹H NMR (300 MHz, Acetone) δ 9.41 (s, 1H), 9.21 (d, J = 8.5, 1H), 8.58 (d, J = 10.1, 1H), 8.17 (dd, J = 5.7, 8.5, 1H), 7.93 (dd, J = 2.7, 8.0, 2H), 4.86 (s, 3H), 4.09 (d, J = 1.9, 3H).

***N*-Methyl-6-Methoxyquinolinium Nonaflate (NM6MQ-Nf).** 6-Methoxyquinoline (0.3142 g, 1.97 mmol) was added to dry acetone (2mL) and sonicated until completely dissolved. Methyl nonaflate (approximately twofold excess) was added to the solution, and the vial was capped. The 5mL high-pressure vial was heated at 80°C for four hours, after which the contents of the vial were poured into 20 mL of diethyl ether. The resulting solid was filtered, and rinsed with Et₂O. After a hot-filtration with 10mg activated charcoal in ethanol, the product was again precipitated with Et₂O and recrystallized from an ethanol-ether mixture. After drying at 110°C in vacuo over P₂O₅, the desired product (0.701 g, 1.48 mmol, 75.1% yield) was recovered as a fine white powder, mp 83-85 °C. ¹H NMR (300 MHz, Acetone) δ 9.41 (s, 1H), 9.21 (d, J = 8.5,

1H), 8.58 (d, J = 10.1, 1H), 8.17 (dd, J = 5.7, 8.5, 1H), 7.93 (dd, J = 2.7, 8.0, 2H), 4.86 (s, 3H), 4.09 (d, J = 1.9, 3H).

***N*-Methyl-6-Hydroxyquinolinium Hexafluorophosphate (NM6HQ-PF6).** *N*-Methyl-6-

Hydroxyquinolinium Iodide (0.321 g, 1.12 mmol) was dissolved in water (10 mL).

Silver hexafluorophosphate (0.384 g, 1.52 mmol) was likewise dissolved in water (10 mL). After addition of the two solutions, silver iodide precipitated immediately, and the solution was stirred for ten minutes. The resulting solid was filtered and discarded. The mother liquor was concentrated by rotary evaporation and dissolved in 10mL EtOH.

After a hot-filtration with 10mg activated charcoal, the product was precipitated with Et₂O, filtered, and recrystallized from an ethanol-ether mixture. After drying at 110°C in vacuo over P₂O₅, the desired product (0.174 g, 0.570 mmol, 50.9% yield) was recovered as a fine white powder, mp 164-168°C. ¹H NMR (300 MHz, Acetone) δ 10.09 (s, 1H), 9.34 (d, J = 5.0, 1H), 9.10 (d, J = 8.5, 1H), 8.54 (d, J = 9.5, 1H), 8.11 (dd, J = 5.7, 8.5, 1H), 7.92 (dd, J = 2.8, 9.6, 1H), 7.75 (d, J = 2.7, 1H), 4.84 (s, 3H). EIMS, m/z 160.1 (M⁺, 24%), 145.1 (100%), 89.1, 63.1; MS (EI, m/z), calcd. for C₁₀H₁₀NO: 160.076. Found: 160.1.

***N*-Methyl 6-Hydroxyquinolinium Tetrafluoroborate (NM6HQ-BF4).** *N*-Methyl-6-

hydroxyquinolinium iodide (0.235 g, 0.819 mmol) was dissolved in water (10 mL).

Silver tetrafluoroborate (0.197 g, 1.01 mmol) was likewise dissolved in water (10 mL).

After addition of the two solutions, silver iodide precipitated immediately, and the solution was stirred for ten minutes. The resulting solid was filtered and discarded. The

mother liquor was concentrated by rotary evaporation and dissolved in 10 mL EtOH. After a hot-filtration with 10 mg activated charcoal, the product was precipitated with Et₂O, filtered, and recrystallized from an ethanol-ether mixture. After drying at 110 °C in vacuo over P₂O₅, the desired product (0.154 g, 0.622 mmol, 75.9% yield) was recovered as white needles, mp 151-152°C. ¹H NMR (300 MHz, Acetone) δ 10.09 (s, 1H), 9.34 (d, J = 5.0, 1H), 9.10 (d, J = 8.5, 1H), 8.54 (d, J = 9.5, 1H), 8.11 (dd, J = 5.7, 8.5, 1H), 7.92 (dd, J = 2.8, 9.6, 1H), 7.75 (d, J = 2.7, 1H), 4.84 (s, 3H). EIMS, m/z 160.1 (M⁺, 24%), 145.1 (100%), 89.1, 63.1; MS (EI, m/z), calcd. for C₁₀H₁₀NO: 160.076. Found: 160.1.

***N*-Methyl-6-Hydroxyquinolinium Hexafluoroantimonate (NM6HQ-SbF₆).** *N*-methyl-6-hydroxyquinolinium iodide (0.123 g, 0.429 mmol) was dissolved in water (10 mL). Silver hexafluoroantimonate (0.223 g, 0.651 mmol) was likewise dissolved in water (10 mL). After addition of the two solutions, silver iodide precipitated immediately, and the solution was stirred for ten minutes. The resulting solid was filtered and discarded. The mother liquor was rotovapped and dissolved in 10 mL EtOH. After a hot-filtration with 10mg activated charcoal, the product was precipitated with Et₂O, filtered, and recrystallized from an ethanol-ether mixture. After drying at 110 °C in vacuo over P₂O₅, the desired product (0.135 g, 0.342 mmol, 79.7% yield) was recovered as a tan-white powder, mp 195-197 °C. ¹H NMR (300 MHz, Acetone) δ 10.09 (s, 1H), 9.34 (d, J = 5.0, 1H), 9.10 (d, J = 8.5, 1H), 8.54 (d, J = 9.5, 1H), 8.11 (dd, J = 5.7, 8.5, 1H), 7.92 (dd, J = 2.8, 9.6, 1H), 7.75 (d, J = 2.7, 1H), 4.84 (s, 3H). EIMS, m/z 160.1 (M⁺, 24%), 145.1 (100%), 89.1, 63.1; MS (EI, m/z), calcd. for C₁₀H₁₀NO: 160.076. Found: 160.1.

***N*-Methyl-6-Hydroxyquinolinium Bis(trifluoromethylsulfonyl) Amide (NM6HQ-N(Tf)₂**. *N*-methyl-6-hydroxyquinolinium iodide (0.125 g, 0.436 mmol) was dissolved in water (10 mL). Silver bis(trifluoromethylsulfonyl) amide (0.202 g, 0.521 mmol) was likewise dissolved in water (10 mL). After addition of the two solutions, silver iodide precipitated immediately, and the solution was stirred for ten minutes. The resulting solid was filtered and discarded. The mother liquor was rotovapped and dissolved in 10 mL EtOH. After a hot-filtration with 10 mg activated charcoal, the product was precipitated with Et₂O, filtered, and recrystallized from an ethanol-ether mixture. After drying at 110 °C in vacuo over P₂O₅, the desired product (0.093 g, 0.21 mmol, 48.2% yield) was recovered as a bright yellow liquid, mp 18-22 °C. ¹H NMR (300 MHz, Acetone) δ 10.09 (s, 1H), 9.34 (d, J = 5.0, 1H), 9.10 (d, J = 8.5, 1H), 8.54 (d, J = 9.5, 1H), 8.11 (dd, J = 5.7, 8.5, 1H), 7.92 (dd, J = 2.8, 9.6, 1H), 7.75 (d, J = 2.7, 1H), 4.84 (s, 3H). EIMS, m/z 160.1 (M⁺, 24%), 145.1 (100%), 89.1, 63.1; MS (EI, m/z), calcd. for C₁₀H₁₀NO: 160.076. Found: 160.1.

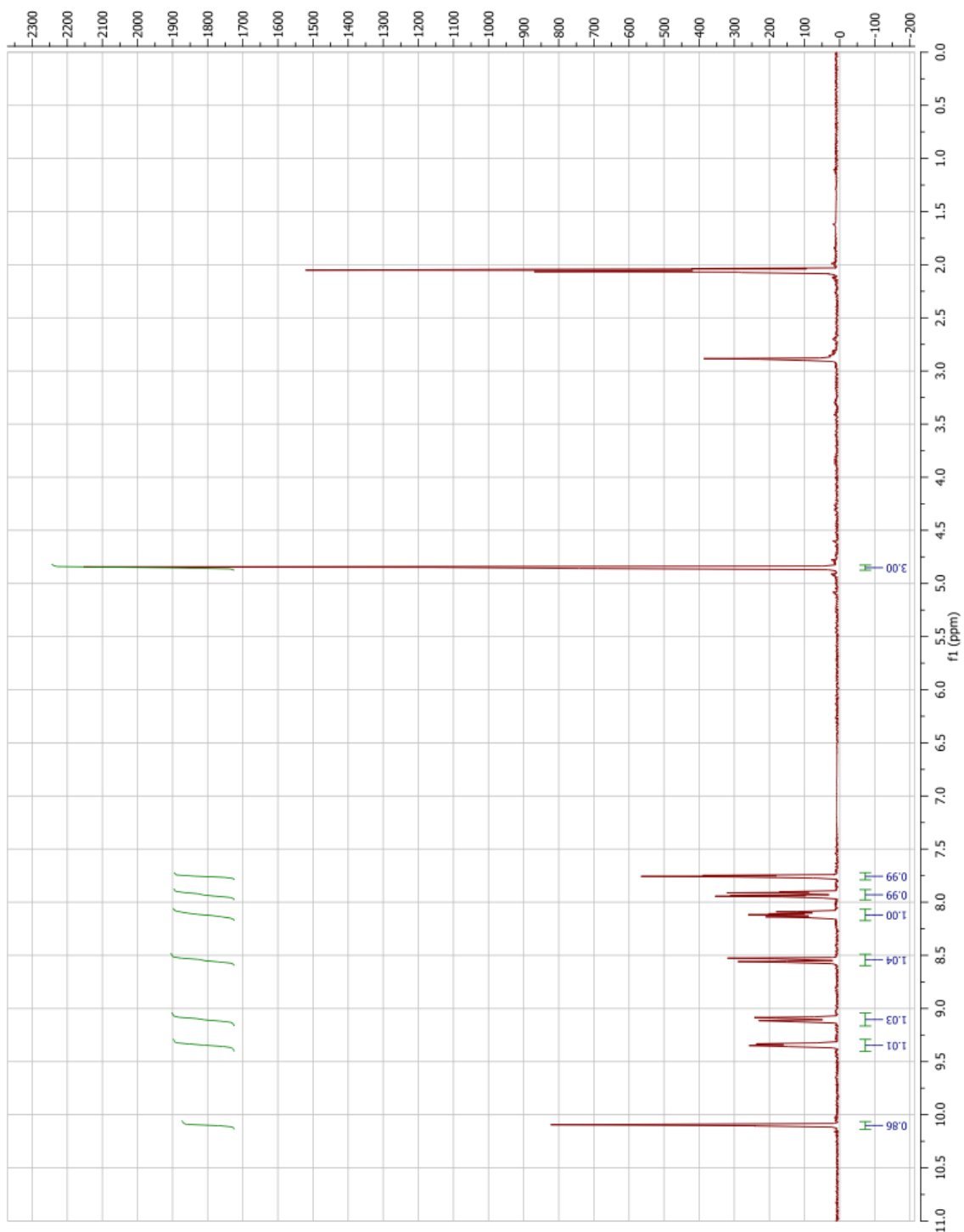


Figure 2.4 ^1H NMR spectrum of NM6HQ-Nf. All NM6HQ compounds of this class share the same proton spectrum.

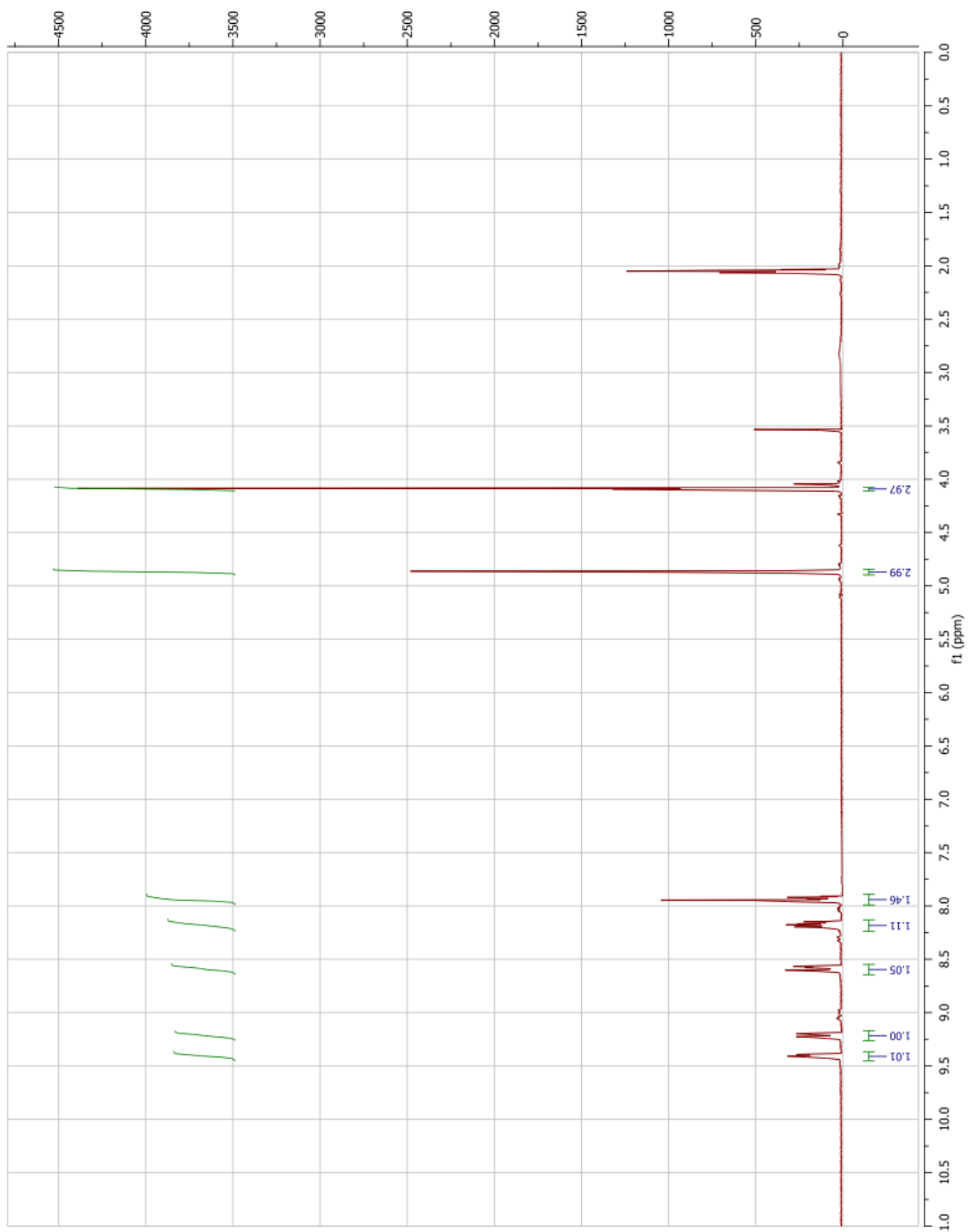


Figure 2.5 ^1H NMR spectrum of NM6MQ-Nf. All NM6MQ compounds share the same proton spectrum.

CHAPTER 3

SPECTROSCOPY OF NM6HQ DERIVATIVES

The previous two chapters have laid the groundwork behind the rational design of photoacids. Fluorescence spectroscopy has historically been the principal method in the study of ESPT, so it is a logical starting point for the photophysical investigations of fluorescent photoacids.

Initial investigations into the photochemistry of **NM6HQ** were undertaken in alcohols for several reasons. Despite acting having a comparable nucleophilicity to water, alcohols are less capable of accepting protons resulting from ESPT. This is partially due to the larger steric bulk of the alcohols compared to water; the bulkier alkyl chains slow proton transfer times due to increased solvent reorganization times while the photoacid is undergoing a light-induced geometric change. Thus, proton transfer can be observed on the picosecond, rather than the femtosecond timescale. This was necessary due to equipment limitations.

All of the **NMH6Q** derivatives synthesized show spectroscopically sufficient solubility in the shorter-chain alcohols, water, DMF, DMSO and acetonitrile. None of these salts are soluble in non-polar solvents which are immiscible with water, except for the few which were soluble in long-chain alcohols. Further details can be seen in **Table 3.1**.

Table 3.1 Solubility of **NM6HQ** salts in solvents of spectral interest. “+” denotes solubility greater than 1.0×10^{-5} M solubility and “O” denotes less than 1.0×10^{-5} M solubility.

Solubility	NM6HQ-I	NM6HQ-Br	NM6HQ-Tf	NM6HQ-Nf	NM6HQ-SbF6	NM6HQ-BF4	NM6HQ-PF6	NM6HQ-N(Tf)2
Acetone	0	0	+	+	0	0	+	+
Acetonitrile	+	+	+	+	+	+	+	+
Chloroform	0	0	0	0	0	0	0	0
Dichloromethane	0	0	0	0	0	0	0	0
Dimethylformamide	+	+	+	+	+	+	+	+
Dimethylsulfoxide	+	+	+	+	+	+	+	+
Dioxane	0	0	0	0	0	0	0	0
Ethyl Acetate	0	0	0	0	0	0	0	0
Hexane	0	0	0	0	0	0	0	0
Toluene	0	0	0	0	0	0	0	0
Water	+	+	+	+	+	+	+	+
Methanol	+	+	+	+	+	+	+	+
Ethanol	+	+	+	+	+	+	+	+
Propanol	+	+	+	+	+	+	+	+
Butanol	+	+	+	+	+	+	+	+
Pentanol	+	+	+	+	+	+	+	+
Hexanol	+	+	+	+	+	+	+	+
Heptanol	+	0	+	+	0	0	+	+
Octanol	+	0	+	+	0	0	+	+

UV-Visible Spectroscopy and Discussion

Ultraviolet and visible spectra were acquired with a Perkin-Elmer Lambda 19 spectrometer equipped with UVWinLab acquisition software. All samples were prepared in the highest quality spectral-grade solvents available from Acros Organics. Solvents were examined prior to use, and were found to have no fluorescent contaminants and a low water concentration.

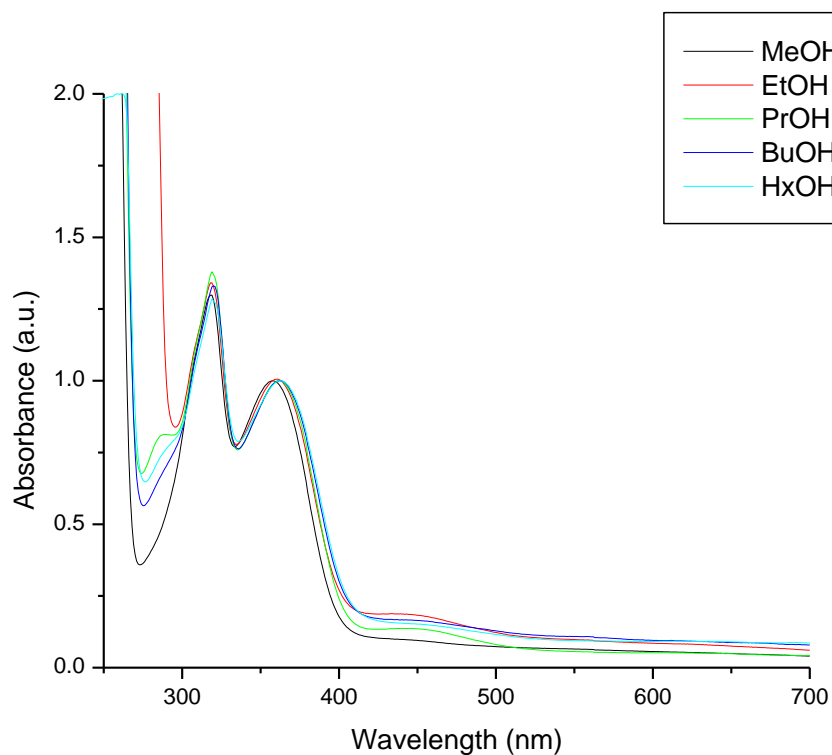


Figure 3.1 Absorbance measurements of **NM6HQ-Nf** in common alcohols. Spectra have been normalized at the lowest energy absorbance (358-364 nm).

Table 3.2 Solvatochromism of **NM6HQ** (all salts) in alcohols C₁-C₈.

Solvatochromism	
Solvent	λ_{max} (nm)
Methanol	358
Ethanol	362
Propanol	362
Butanol	364
Pentanol	364
Hexanol	364
Heptanol	364
Octanol	362

Representative ultraviolet-visible absorbance measurements are shown in **Figure 3.1**. Although ground-state deprotonation should not occur in alcoholic solvents due to **NM6HQ**'s ground state pK_a below that of the alcohols tested, a small amount is seen regardless. Ground-state deprotonation is evidenced by a broad absorption centered near 420 nm, and a narrow feature at approximately 275 nm. In all cases and in all future fluorescence studies examining the effects of proton transfer, the ground-state deprotonation was considered, and never exceeded 1%. Ground state deprotonation in alcohols seems to be correlated with the concentration of the sample.

All **NM6HQ** salts exhibit a small negative solvatochromatic effect in the solvents tested (**Table 3.2**).

Steady-State Fluorescence Spectroscopy

While no differences were seen in the absorption spectra between **NM6HQ** salts with different anions in alcohols, the steady-state fluorescence spectra tells a different story. **Figure 3.2** shows the pathways of fluorescence decays during proton transfer in

the photodissociation process. “C” and “C*” refer to protonated cation in the ground and excited state, respectively. “Z” and “Z*” refer to the deprotonated zwitterion in the ground and excited state, respectively.

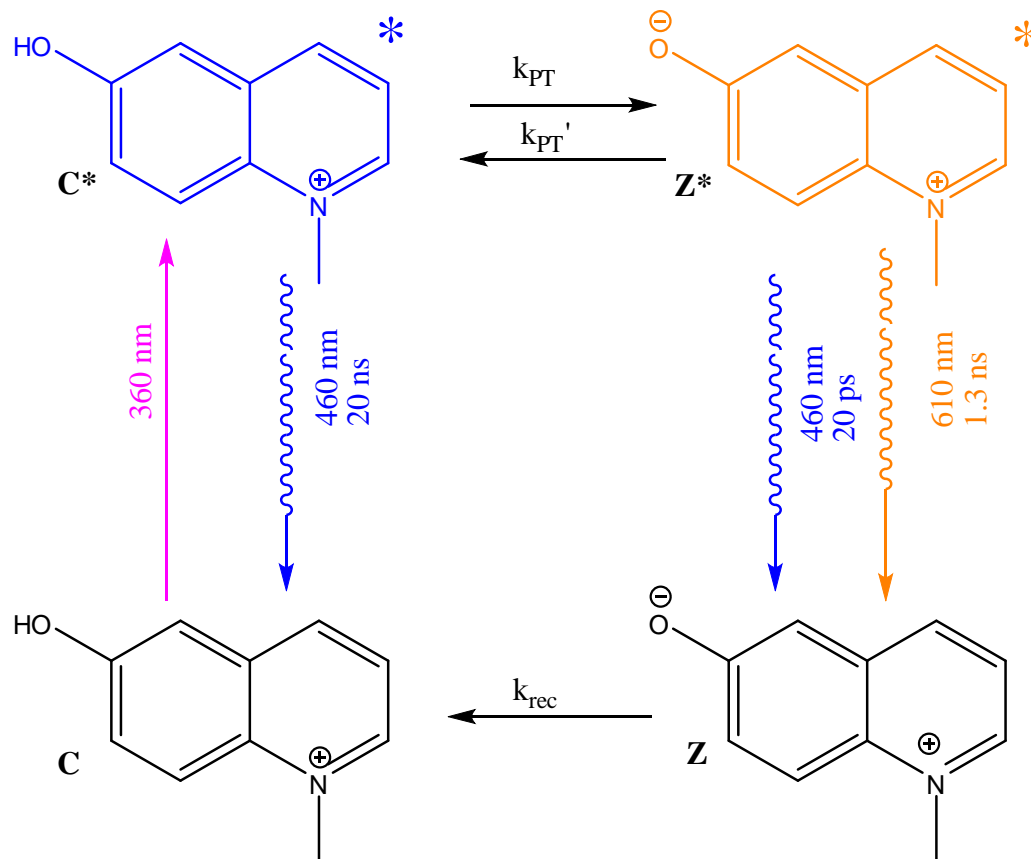


Figure 3.2 Schematic diagram showing the proton transfer and recombination and fluorescence decay pathways for **NM6HQ**.

Steady-state fluorescence spectra were measured on a SPEX Fluorolog 112X spectrofluorimeter utilizing the DataMax software package. Spectra were collected at a right angle from the excitation source. The excitation source was a 1000 W high-pressure Hg-Xe lamp. Entrance and exit slits were set to 1.5 mm. The same samples for absorbance and fluorescence were used, and were of a concentration between 10^{-4} to 10^{-5} M. All spectra were collected in quartz cuvettes. Unless otherwise specified, all samples

were collected in solvents that were not pH-controlled and collected at room temperature and pressure. Fluorescence emission spectra were collected at the wavelength of the longest maximum absorption and were corrected accordingly.

Fluorescence Behavior in Alcohols

The results of steady-state fluorescence acquisitions are displayed in **Figure 3.3**. Spectra in this diagram have been normalized at 436 nm to make a comparison between fluorescence from the protonated **C*** and deprotonated **Z*** hydroxyquinolinium cation. **NM6HQ-Nf** was used for this experiment, since it has exhibited the strongest proton transfer to solvent (PTTS), in addition to lacking a heavy-ion effect which quenches fluorescence, which the iodide and bromide salt may exhibit.

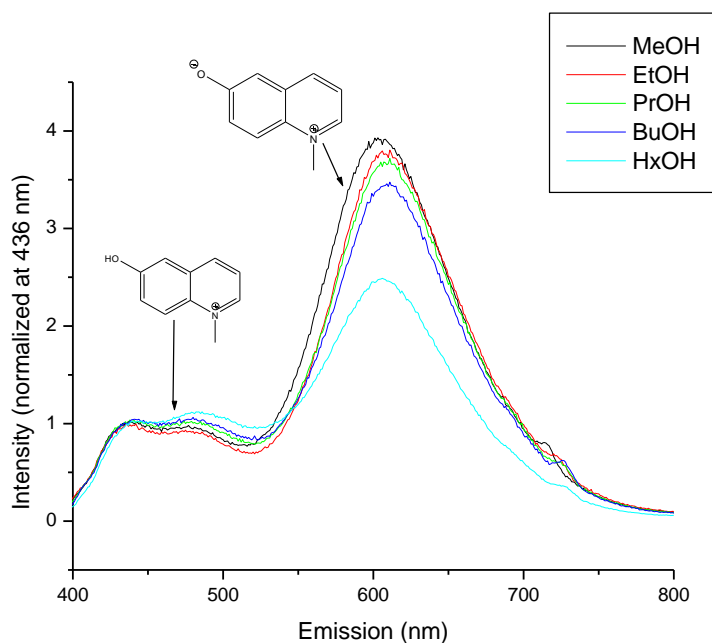


Figure 3.3 Steady state fluorescence of **NM6HQ-Nf** in selected alcohols.

The broad emission centered at 460 nm corresponds to fluorescence from the protonated cation (\mathbf{C}^*), and the peak at 610 nm is the emission from the deprotonated zwitterion (\mathbf{Z}^*). By comparing of the intensities of the fluorescence emissions of \mathbf{C}^* and \mathbf{Z}^* , it is apparent that proton transfer occurs more readily in the shorter chain alcohols. Despite the fact that increasing alkyl chain length on the alcohols provides each longer-chain alcohol an incrementally more basic character, proton transfer is most readily seen in the shorter alcohols. This is due to a faster reorganization time of the solvent cage surrounding the fluorophore to accept the proton more readily.

Steady-State Fluorescence Profiles of Varying Anions

Steady-state fluorescence spectra of **NM6HQ** salts with different anions exhibited unpredictable results. **Figure 3.4** gives an overview of the profile of **NM6HQ** with different anions in butanol. Butanol was chosen for the reason that time-resolved measurements in butanol were compatible with the picosecond instrumentation available.

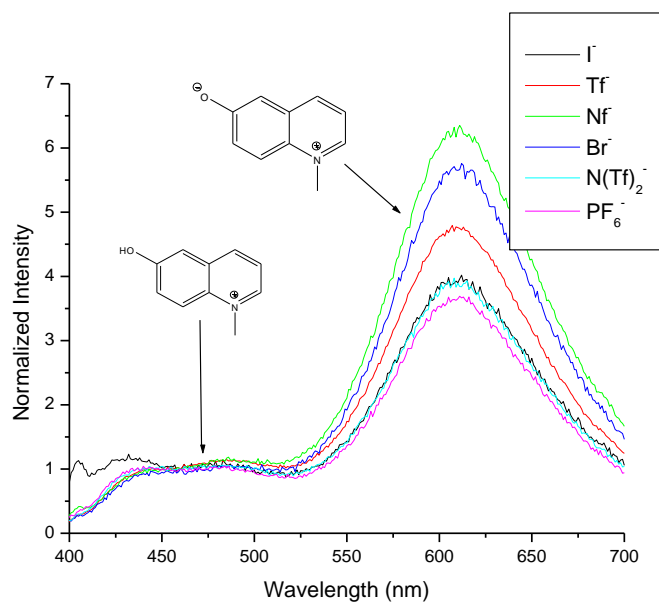


Figure 3.4 Steady-state fluorescence (normalized at 460 nm) spectra of varying counterions of **NM6HQ** in butanol (note that SbF_6 and BF_4 were omitted and will be discussed later).

NM6HQ-Nf was shown to exhibit the largest proton transfer to solvent. Since none of the corresponding counterions is more nucleophilic than the solvent (protonated butanol having a $\text{p}K_a$ of $-2.39^{[27]}$), a possible explanation lies in that the counterion may be interfering with the solvent cage reorganization of butanol as the hydroxyquinolinium cation is excited from ground state to its excited-state geometry.

This effect is seen even more intensely when comparing the **C*** to **Z*** ratios of fluorescence intensity for very weakly nucleophilic counterions. **Figure 3.5** demonstrates this principle. Despite the fact that the same iodide salt (which shows a strong proton transfer to solvent) was used in the synthesis of all silver anion-metathesis salts, the tetrafluoroborate and hexafluoroantimonate exhibited a marked increase in fluorescence from the cation peak and conversely a diminished emission from the zwitterion. This will be discussed later in the chapter.

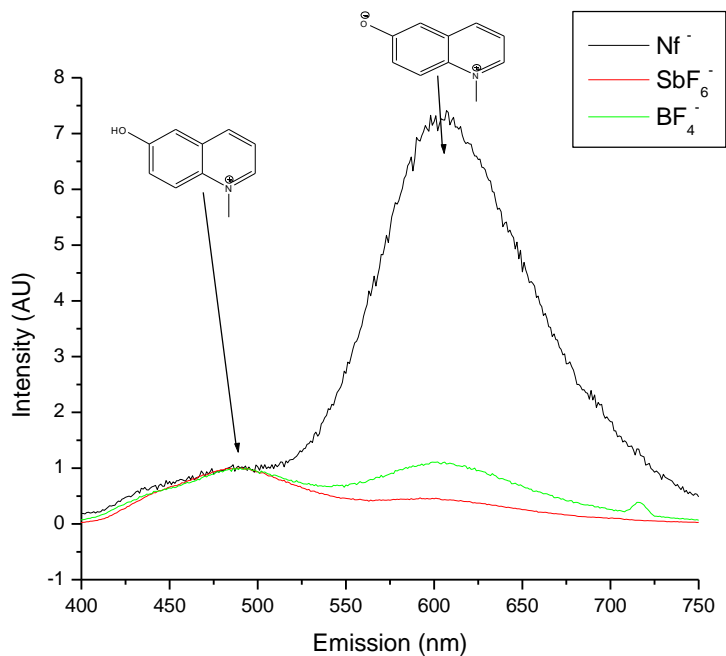


Figure 3.5 A steady-state comparison of three **NM6HQ** compounds with drastically different fluorescence properties. Peaks are normalized at 460 nm.

Using butanol solvent as a benchmark solvent for proton transfer in these experiments, a ratiometric table of fluorescence intensities is provided below as an approximate estimate of excited-state proton transfer efficiency.

Table 3.3 A ratiometric comparison estimating proton transfer capabilities by comparing peak ratios

	$I_{Z(610\text{ nm})}/I_{C(460\text{ nm})}$
BF₄⁻	1.45
Br⁻	5.65
I⁻	3.90
Nf⁻	8.89
N(Tf)₂⁻	3.90
PF₆⁻	3.65
SbF₆⁻	0.56
Tf⁻	4.76

Table 3.3 shows that **NM6HQ-Nf** clearly exhibits the strongest proton transfer to butanol since the ratio of **Z*** to **C*** is the largest, suggesting maximal proton transfer to solvent.

Fluorescence Lifetime Measurements

Lifetime measurements were conducted in butanol. Each time-resolved single photon counter (TRSPC) spectrum was taken from the exact sample corresponding to the sample described in the UV/Vis and steady-state sections earlier.

The instrument in use was the LifeSpec TRSPC setup available in the Dickson Lab. A picosecond pulse dye laser providing 372 nm excitation was used as the light source. In butanol, this excitation overlaps the lowest energy absorption and excitation peaks. A high speed microchannel plate photomultiplier tube (Hamamatsu R3809U-50) cooled to -20 °C to reduce noise was utilized as the detector. The pulses were communicated to a hardware controller by a constant fraction discriminator (CFD). A second CFD was used to obtain a timing reference pulse from the light source. The time-amplitude-converter output voltage was sent through a biased amplifier with a variable gain and a variable offset. Subsequently, the amplified signal was fed to the analog-to-digital converter. Finally, a multichannel analyzer software (Edinburg Instruments F900) was used to process the signal and convert it to a PC format. The Instrument Response Function (IRF) of the TRSPC setup is typically in the range of 20 ps to 30 ps. Titanium dioxide and non-dairy creamer dissolved in water acted as the light-scattering samples.

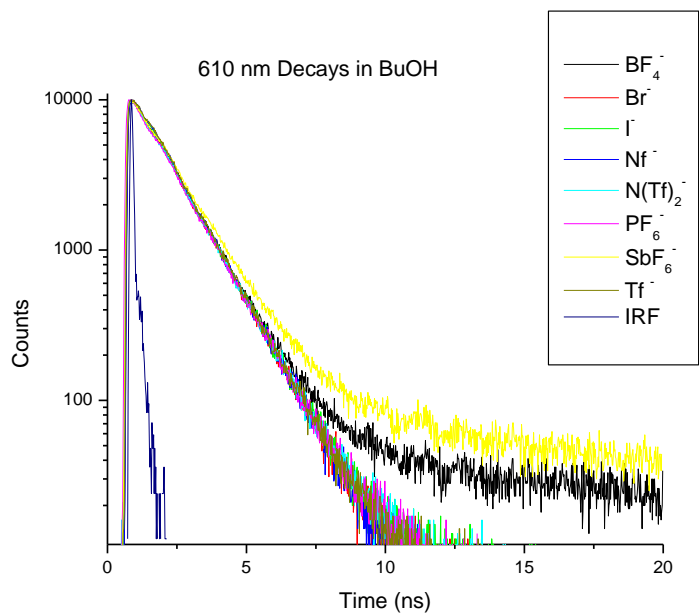


Figure 3.6 **NM6HQ (Z*)** decays in BuOH for all synthesized counterions (372 nm excitation). **NM6MQ** results not reported because decay at 610 nm is neither possible nor observed.

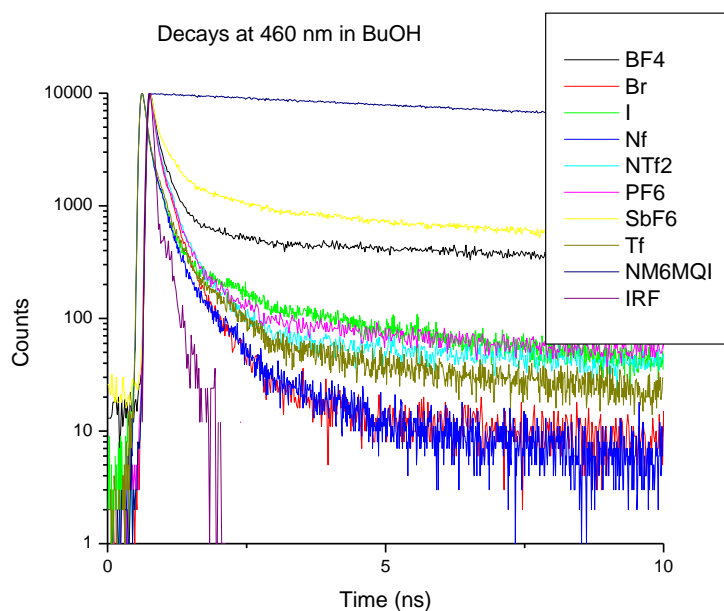


Figure 3.7 **NM6HQ (C*)** decays in BuOH at 460 nm (372 nm excitation).

Fluorescence lifetime data was fitted using the program FFIT, written by N. Tkachenko in 1995. Spectra were corrected with regard to the instrument response function.

Decays from **Z*** at 610 nm show a single-exponential decay with a lifetime of 1.3 ns. Samples which fluoresce strongly from **C*** (**NM6HQ BF4** and **SbF6**) band at 460 nm show a tailing peak with a lifetime of 20 ns. This tail is seen even at 610 nm (**Figure 3.6**).

The fluorescence at 460 nm from **C*** shows a multi-exponential decay, with the fluorescence heavily dependent on the counterion (**Figure 3.7**). An initial quick decay of 20 ps is seen for compounds which strongly transfer a proton to butanol in the excited state, such as the nonaflate salt. Compounds which do not exhibit strong PTTS with regards to the steady-state spectrum (such as the hexafluoroantimonate salt) show a diminished initial decay at 460 nm from the 20 ps fluorescence of **Z***, demonstrating that they are less capable of donating a proton to butanol. However, these compounds fluoresce strongly from the **C*** at 460 nm. Fluorescence from the cation suggests that proton transfer is could be hindered from inadequate solvation of the counterion.

Behavior in Non-Basic Solvents

Using the same time-resolved protocols outlined earlier, the fluorescence spectra of all **NM6HQ** compounds were measured in acetonitrile. Unlike solvents capable of accepting a proton, no differences were observed in any samples. All samples show consistent fluorescence at 490 nm with a single-exponential lifetime of 20 ns.

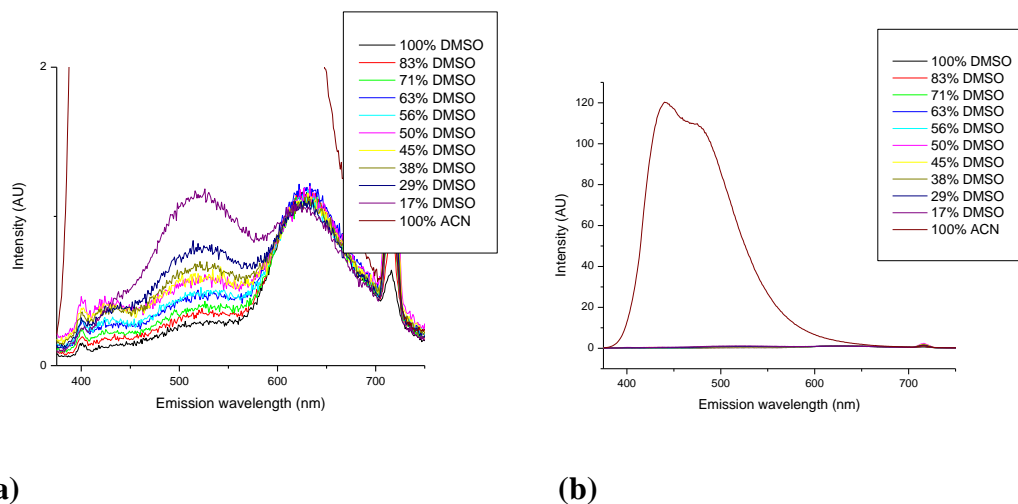


Figure 3.8 Fluorescence in DMSO/ACN mixtures. **Figure 3.8(a)** is a close-up of the region, and **Figure 3.8(b)** is a broad view showing the intensity of the peak at 490 nm.

Figure 3.8 shows the effect of binary solvent mixtures on fluorescence from the C^* and Z^* for **NM6HQ-Nf**. Dimethyl sulfoxide and acetonitrile were chosen because they display opposite behaviors towards excited **NM6HQ**; protonated DMSO has a pK_a of -1.5 and is easily capable of accepting a proton from **NM6HQ** whereas protonated acetonitrile has a pK_a of -15 and incapable of receiving a proton from any **NM6HQ** salt^[28].

Aggregation Studies

One possible explanation behind the differences in fluorescence spectra (and consequently in proton transfer) is that aggregation is a limiting factor. Aggregations have been seen in earlier literature to inhibit proton transfer^[29].

To test this possibility, two separate experiments were undertaken.

Dilution Experiments

First, three salts of the **NM6HQ** class with immensely different fluorescence spectra were examined via spectroscopic means; nonaflate, tetrafluoroborate and hexafluoroantimonate were examined due to their differences in steady-state fluorescence and time-resolved decays. Dilution studies were performed at four different concentrations in methanol and at one concentration in DMSO. In DMSO, all **NM6HQ** salts share similar steady-state fluorescence spectra, suggesting excellent excited-state PTTS. However, the fluorescence spectra in methanol show a large discrepancy. Both solvents are capable of receiving a proton, but the proton transfer is inefficient for methanol, depending on the counterion.

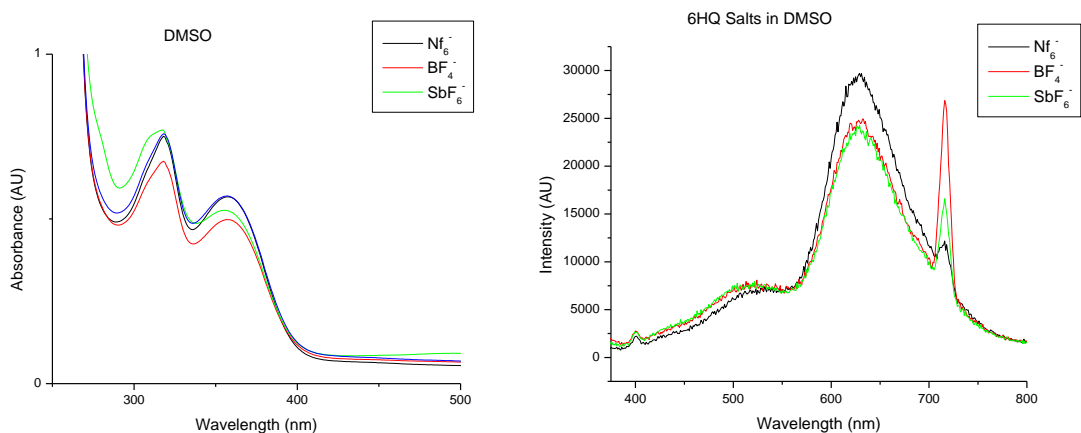


Figure 3.9 Absorbance and fluorescence of samples in DMSO

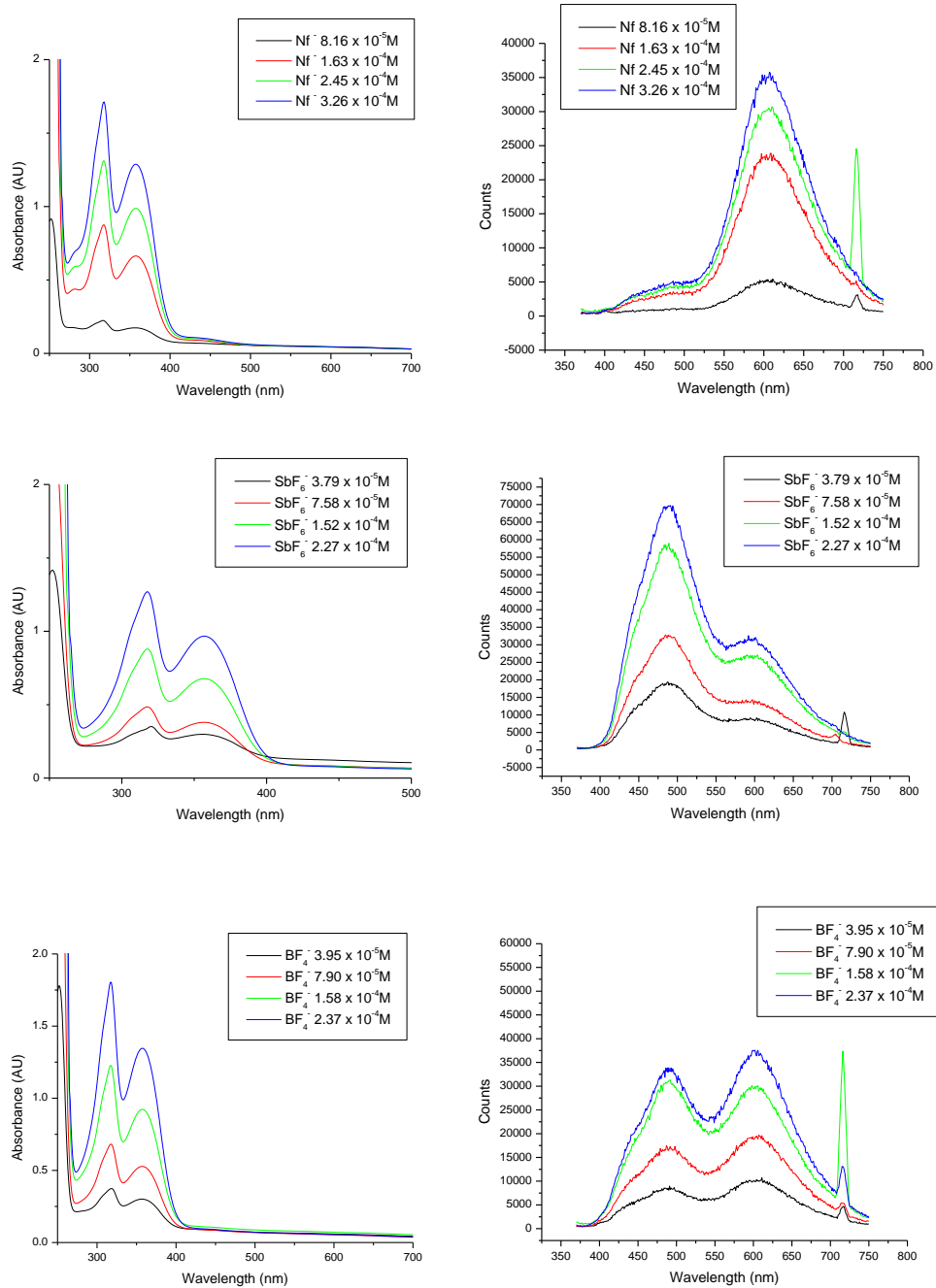


Figure 3.10 Absorbance and fluorescence spectra of three different **NM6HQ** samples at four concentrations in methanol.

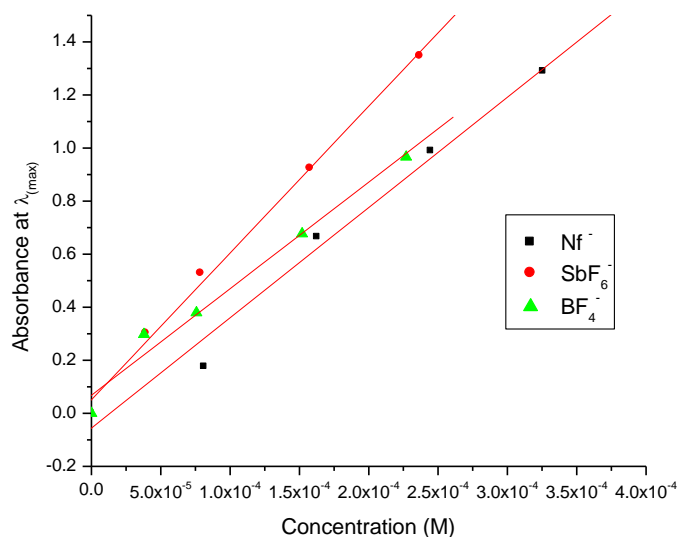


Figure 3.11 Beer's Law plot in MeOH

Figure 3.9 exemplifies the steady-state fluorescence spectra in DMSO. It is noteworthy to observe that all three compounds tested exhibit strong PTTS in this solvent. The situation changes in drastically in **Figure 3.10**, however. In methanol, the ratios between **C*** and **Z*** become painfully apparent. The nonaflate continues to typify strong proton transfer to solvent, whereas the tetrafluoroborate and hexafluoroantimonate salts significantly decrease proton transfer in this solvent. This effect is not dependent on the levels of dilution, and the ratio of **C*** to **Z*** does not change in any of the fluorescence spectra for any concentration tested. These steadfast ratios suggest that aggregation is not a significant factor. **Figure 3.11** further illustrates the fact that aggregation plays an insignificant role. A Beer's Law plot from the lowest energy absorbances at 358 nm show little deviation from linearity.

Dynamic Light Scattering

Initial dilution experiments disagreed with the possibility of aggregation. Therefore, a Dynamic Light Scattering (DLS) was used to check for the formation of aggregates.

The samples used in DLS acquisitions were the same samples prepared in the preceding dilution studies. For the sake of convenience, samples labeled “A” correspond to the most concentrated samples, whereas “D” samples are the most dilute. Measurements were acquired in methanol, and were compared with a blank methanol spectrum.

A Wyatt Technology Dynapro Titan instrument, available in the Lyon laboratory, was used for the measurements. The instrument was equipped with a 784 nm light source, and cumulants were fit to a monomodal dispersion model. Cumulants were collected over a 100 second time frame at intervals of ten seconds each.

Table 3.4 Light scattering data. “R” is the average particle radius, and “MW” is the estimated molecular weight of the particles based on protein aggregates of similar particle radius. The samples range from “A” (most concentrated) to “D” (least concentrated).

	R (nm)	MW (kDa)
MeOH Blank	1.13E-01	0.02062
Nonaflate A	7.68E+03	5.35E+09
Nonaflate B	1.26E+00	77.39
Nonaflate C	9.60E-01	23.45
Nonaflate D	7.85E-02	0.0149
BF ₄ A	1.37E+03	7.29E+07
BF ₄ B	1.79E-01	1.86E+06
BF ₄ C	5.44E-02	0.211
BF ₄ D	2.15E+02	0.003701
SbF ₆ A	8.46E+03	1.83E+12
SbF ₆ B	3.40E+03	6.38E+10
SbF ₆ C	2.32E+00	5.57E+09
SbF ₆ D	1.75E-01	441

While prior experiments suggested that scattering was not occurring, **Table 3.4** points to an inconclusive possibility that aggregation could be occurring. However, the amount of scattering seems to bear no correlation to ESPT in MeOH.

All samples showed greater light scattering than the methanol blank. For instance, “Nonaflate A” was the one of the most concentrated samples tested. It showed the most efficient proton transfer to solvent despite the fact that scattering shows a large average particle size and high calculated molecular weight. This scattering amount was even greater than the most dilute sample “SbF₆ D”, which did not show efficient proton transfer even in dilute methanol. This suggests that even though aggregation may be occurring, it is neither hindering nor assisting proton transfer in methanol.

These two experiments dictate that aggregation and consequently diminished proton transfer is not likely to affect ESPT in MeOH. Another explanation is needed.

Counterion Discussion

Because several of the non-nucleophilic counterion salts were synthesized directly from the same samples of **NM6HQ-I** which were used from spectroscopy by anion metathesis, there was no possible means of molecular modification to the **NM6HQ** ring. Contamination was avoided by thorough purification, and final products were confirmed by NMR and MS in addition to UV-Vis spectroscopy. The only difference lies in the counterion and as seen in fluorescence spectroscopy, the counterion has significant influence in the photochemistry of the system.

A decisive conclusion has not been reached yet, however there is one experiment and three possibilities worth mentioning.

Upon addition of two molar equivalents of tetrabutylammonium hexafluoroantimonate ($N^+(C_4H_9)_4 SbF_6^-$), to a spectroscopic sample of **NM6HQ-Nf**, no increase whatsoever in the fluorescent emission peak at 460 nm was seen. This suggests

that the counterion could be playing a role in accepting, and possibly even facilitating the dissociation of the proton.

A second possibility is the disruption of the solvent cage by the counterion to hinder ESPT, but this explanation is discouraged by the prior experiment.

Finally, a possibility based upon Marcus Theory electron transfer may provide an answer. The cationic quaternary quinolinium could act as a mild photo base upon excitation, and could in theory incorporate an electron into the molecular orbital depending on the oxidation potential of the counter ion. A mathematical treatment of this nature is beyond the scope of this thesis and is a study unto itself in ion-pairing mathematics.

CHAPTER 4

CATIONIC POLYMERIZATION THROUGH DIRECT ESPT

NM6HQ salts have shown their capability of PTTS in several basic solvents. Despite this observation, other compounds capable of ESPT have not decisively initiated chemical reactions via a proton transfer mechanism. Much speculation surrounds several compounds which claim this ability. This chapter begins with an overview of literature claiming photochemical reactions initiated by excited-state proton transfer before demonstrating that the investigated **NM6HQ** salts are in fact capable of initiating photochemical reactions via ESPT.

Background Information

Dimethyl-4-hydroxyphenylsulfonium hexafluoroantimonate

A 1980 paper claiming reversible proton transfer from a hydroxyphenyl sulfonium^[30] was published. This paper claims that the hydroxyl proton is responsible for the photoinitiation, and the supposed mechanism is shown in **Figure 4.1**.

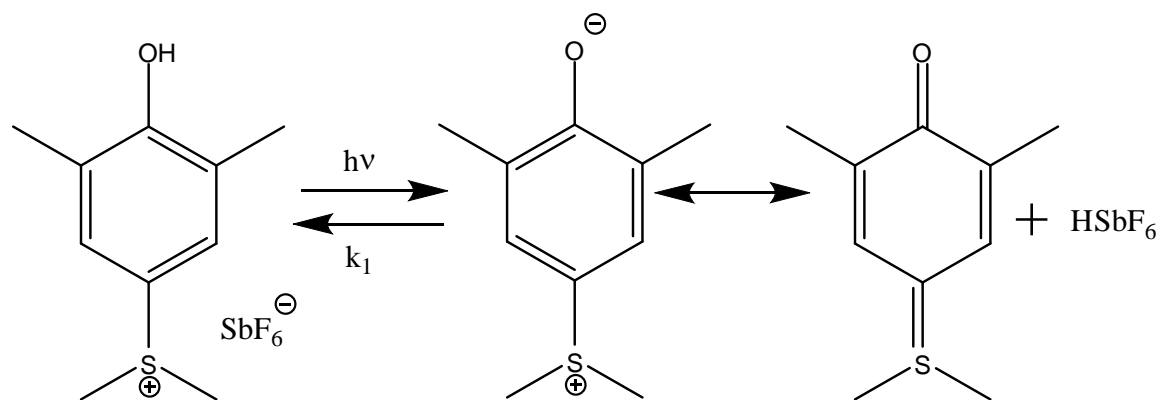


Figure 4.1 Claimed mechanism of photoinitiation via a 4-hydroxyphenylsulfonium salt^[30].

The field of PAGs has abundant literature dealing with sulfonium salts. These compounds generate acid based in a generally agreed-upon decomposition mechanism seen later in **Figure 4.6**. Numerous dimethylsulfonium salts lacking a 4-hydroxyl have been shown to act as PAGs^[31-33]. Additionally, the 4-methoxy- derivative has two outstanding patents as a cationic photoinitiator, and shows a polymerization rate similar to dimethyl-4-hydroxyphenylsulfonium^[34, 35].

Fluorinated Phenols

Recent literature has claimed that fluorinated phenols such as pentafluorophenol are capable of initiating photopolymerizations^[11]. Although pentafluorophenol was successful in inducing deuterium exchange with acetone in this laboratory, the experiment of polymerizing an epoxide could not be duplicated. Even if these compounds did successfully initiate reactions, it has been shown that hydrolysis of the carbon-fluorine bond could be a possible photochemical outcome, thereby generating

hydrofluoric acid^[36]. This lends skepticism to the claim of proton transfer being the only method of initiating the reaction in pentafluorophenol

Hydroxymethylphenols

Hydroxymethylphenols (**Figure 4.2**) have been claimed to selectively cleave protecting groups from organic compounds^[33]. While the authors present a novel use for photoacid chemistry, it is doubtful that their initiation occurs at 365 nm as the paper claims. Phenols tend to absorb light well below 300 nm. At best, molecular orbital calculations indicate that this compound will exhibit very weak ESPT. It should not act as a “super” photo acid, thereby limiting potential applications.

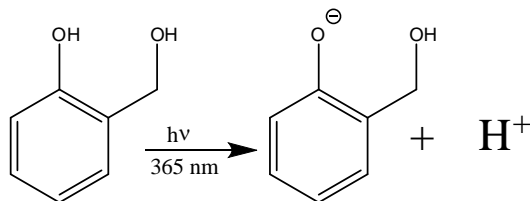


Figure 4.2 Hydroxymethylphenol photoacid.

In each of these studies, it is sheer speculation that proton transfer from a phenolic moiety is initiating the reactions investigated; none of the studies have taken measures such as synthesizing derivatives incapable of ESPT (for example, methoxy- derivatives), nor have they examined the possibility of irreversible acid generation through photodegradation. The studies performed in this chapter aim to demonstrate that proton transfer alone is responsible for the photoinitiation of cyclical epoxy monomers in the **NM6HQ** derivatives.

NM6HQ: Excited-state proton exchange with acetone

Although proton was not directly observed with any of the NM6HQ analogues in acetone or acetonitrile via the fluorescence decay of the excited zwitterion typically appearing at 610 nm, a possibility remains that the Z^* is formed, albeit on a time scale not observed by the optical instrumentation utilized in Chapter 3. As such, NMR serves as a useful tool for monitoring slow reactions that occur over the course of several hours or days.

If ESPT is in fact taking place in acetone, this would suggest that the carbonyl on acetone is protonated, allowing for an acid-assisted deuterium exchange. An exchange of this nature infers that the excited-state pK_a of the compound being tested is somewhere on the order of -7, the pK_a of protonated acetone^[28]. Not only would this signify the lowest excited-state pK_a reported in literature, it also would signify the largest pK_a jump observed to date.

Although the mechanism has not been confirmed, a likely possibility is proposed in **Figure 4.3**.

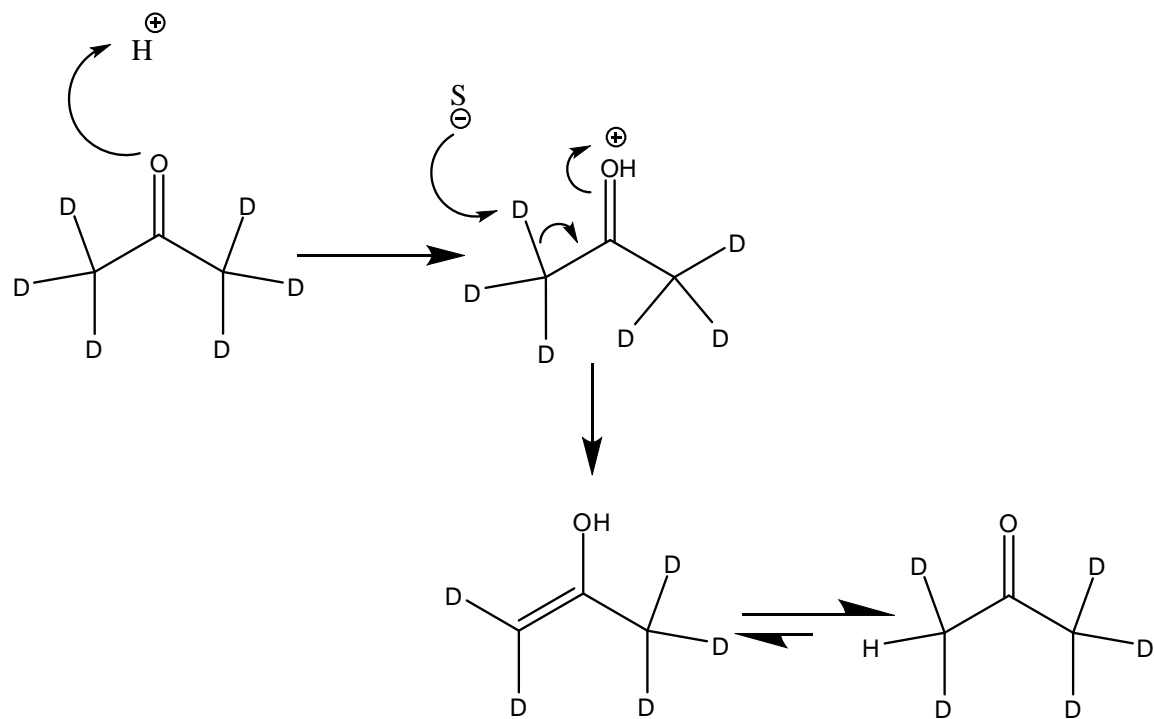


Figure 4.3 Proposed mechanism for hydrogen-deuterium exchange. “S” refers to a nucleophile, either a solvent molecule or the counter-ion.

NM6HQ-Nf (0.0093 g, 0.020 mmol) was dissolved in 0.75 mL d_6 acetone (99%, Cambridge Isotope Laboratories). The contents were capped in an NMR tube. Photoirradiation was carried out with a Hanovia water-cooled 450 W high pressure mercury lamp. A high bandpass filter (borosilicate glass) ensured that wavelengths below 310 nm were filtered. The experiment was conducted at room temperature, and the photochemical reaction was monitored periodically by NMR.

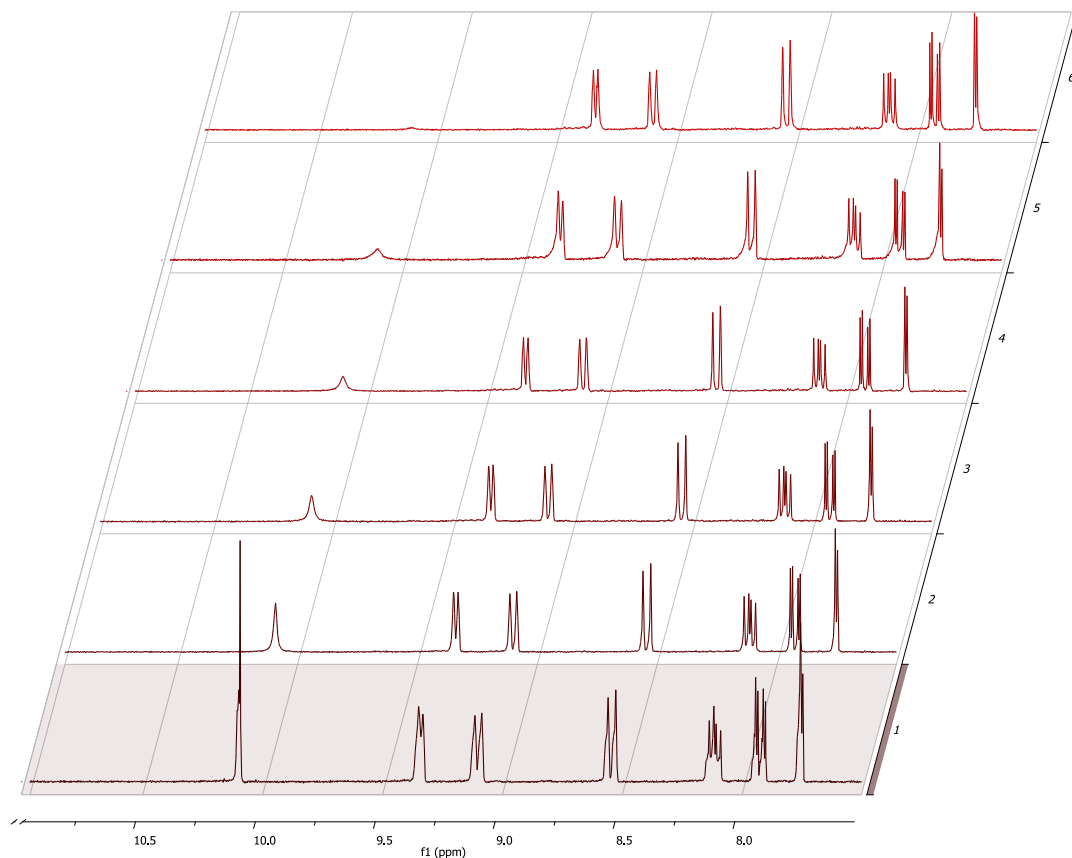


Figure 4.4 ^1H NMR of NM6HQ-Nf in d_6 -acetone. Times are initial- immediately following preparation (1), 2 hours (2), 4 hours (3), 6 hours (4), 8 hours (5) and 12 hours exposure.

In **Figure 4.4**, the proton signal from the hydroxyl peak at 10.15 ppm decreases following exposure in the photoreactor. This diminution does not occur when the sample preparation is kept in the dark for up to 72 hours, which was the longest period of time that dark sample preparations were monitored. This suggests that the excitation source is necessary to force hydrogen-deuterium exchange with acetone. **Figure 4.5** shows the ratios of the hydroxyl peak (10.123-10.080 ppm) to the integration of the unchanging methyl peak intensity (4.875-4.826 ppm).

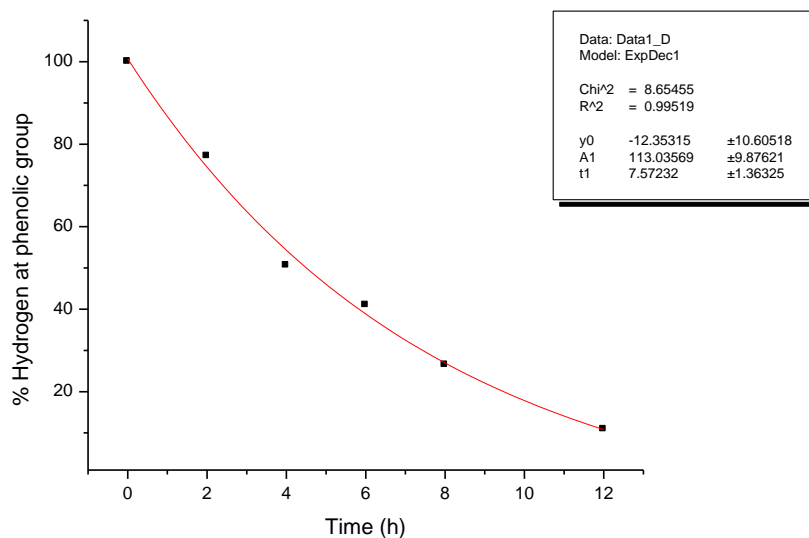


Figure 4.5 Proton exchange with acetone for NM6HQ-Nf.

Polymerization with PAGs

Since NM6HQ-Nf was observed to transfer a proton to acetone resulting in deuterium exchange, it is logical to utilize this property to initiate an acid-catalyzed reaction to further illustrate its capabilities.

Photoacid generators (PAGs) are employed in industrial applications as a means of controlling polymerization through photo induced acid generation. Several types of photoacid generators, specifically cationic initiators have been examined, and the majority of them are comprised of aryl onium salts, specifically from the iodonium, sulfonium, phosphonium and diazonium classes^[10]. While the mechanism for acid generation for these compounds is disagreed upon, it is clear that they do not initiate polymerizations by direct proton transfer. Rather, the polymerizations are initiated through protons generated from photoinitiated decomposition of the PAG, in the presence of trace amounts of water in the polymer/PAG blend^[37] as **Figure 4.6** shows.

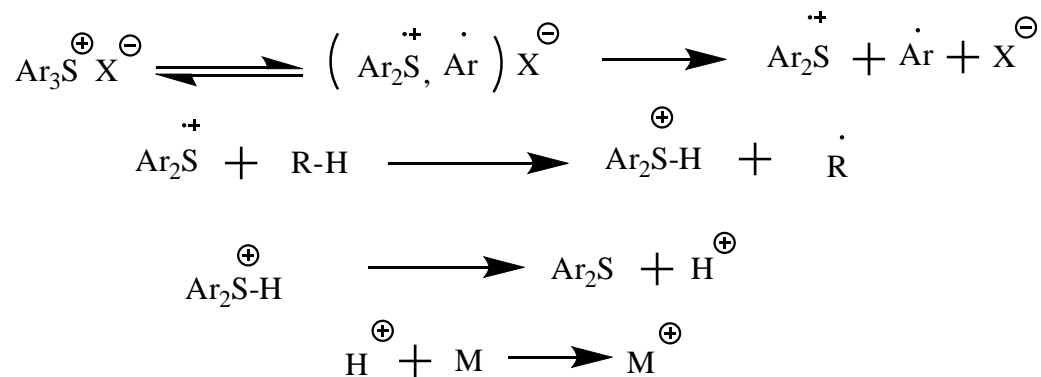


Figure 4.6 Mechanism of onium acid generation using a sulfonium salt as the cationic initiator

Polymerization due to direct proton transfer rather than proton abstraction could confer several advantages. The pH of the reaction may be controlled more easily through light rather than through addition of a base. With ESPT, acid generation should be transient, and the system should revert back to its starting pH if the system works ideally. The ability to incorporate deuterium or tritium into specific sites exists. Finally, the biaryl hydroxyl aromatic systems utilizes another unique feature, in that proton transfer and thus acid generation is capable at longer wavelengths.

In traditional PAGs, short wavelength UV light is often used to initiate polymerizations because aryl onium initiators have their principal absorption bands in the short wavelength of the UV spectrum. However, some uses require a longer wavelength of light to initiate polymerizations such as printing and dental applications^[38].

Traditional onium PAGs have not been observed to undergo photodegradation into acids at wavelengths typically above 320 nm, despite modifications to the aryl onium substituents to favor longer wavelengths^[39]. Onium salts tend not to photolyse under long wavelength conditions regardless of the substituents and despite much synthetic effort. A method of enabling long-wavelength photoinitiation is through the use of

photosensitizers, although this additional component adds complexity to the system. Photosensitizers are generally toxic and exhibit poor solubility; these are factors to consider in addition to finding the optimum ration of PAG to sensitizer. From what we have seen, **NM6HQ** salts initiate proton transfer to solvent with as high as 400 nm excitation, the beginning of the visible spectrum.

To investigate whether polymerization via direct-proton transfer was possible for **NM6HQ-Nf**, experiments were conducted on three monomers: cyclohexene oxide (**CHO**), dicyclopentadiene diepoxide (**DCPDE**), and bisphenol A diglycidyl ether (**BADGE**). These compounds are displayed in **Figure 4.7**.

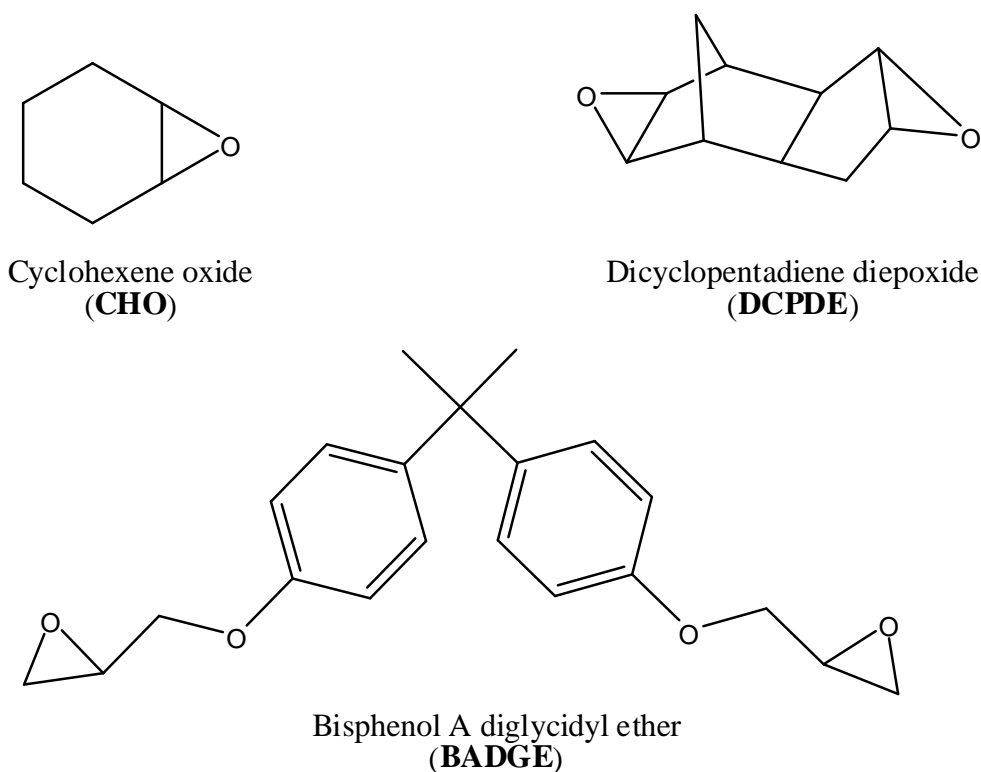


Figure 4.7 Monomers investigated for ESPT initiated cationic polymerization.

Polymerization Experiments

All **NM6HQ** salts (approximately 1 mg of each) were dissolved in 0.75 mL d_6 acetone (99%, Cambridge Isotope Laboratories). Cyclohexene oxide (20 μ L) was added to the NMR tube, creating approximately a 5% (w/w) sample of photoacid to substrate. The contents were capped in an NMR tube. Photoirradiation was carried out with a 450W Hanovia water-cooled high pressure mercury lamp. A high bandpass filter (borosilicate glass) ensured that wavelengths below 310 nm were blocked. The experiment was conducted at room temperature. NMR spectra were recorded typically at 2h intervals. Rates of polymerization were determined by calculating the constant integration of peaks between 1.0-1.5 ppm to the disappearance of the peak at 3.05 ppm. This peak at 3.05 ppm is indicative of the proton alpha to the epoxide.

Cyclohexene Oxide

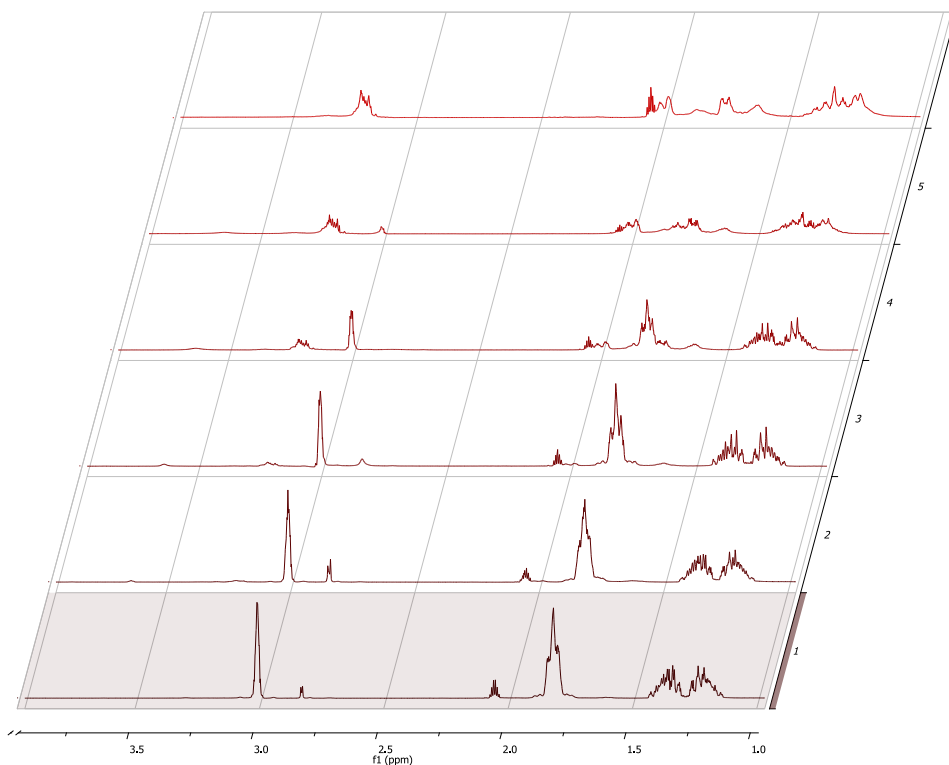


Figure 4.8 Photopolymerization of **CHO** with **NM6HQ-Nf** over 15 h in a photoreactor. Times: initial (1), 1 hour (2), 2 hours (3), 4 hours (4), 6 hours (5), 15 hours (6).

Initial polymerizations were attempted with **CHO** for several reasons; it is fairly sensitive to acid generation at room temperature, it is an industrial and academic standard for testing cationic photoinitiators, and literature is replete with examples for comparison.

An example polymerization NMR spectrum with respect to time is given by **Figure 4.8**. This figure utilizes the best photoacid synthesized, **NM6HQ-Nf** as the photoacid generator in the experiment.

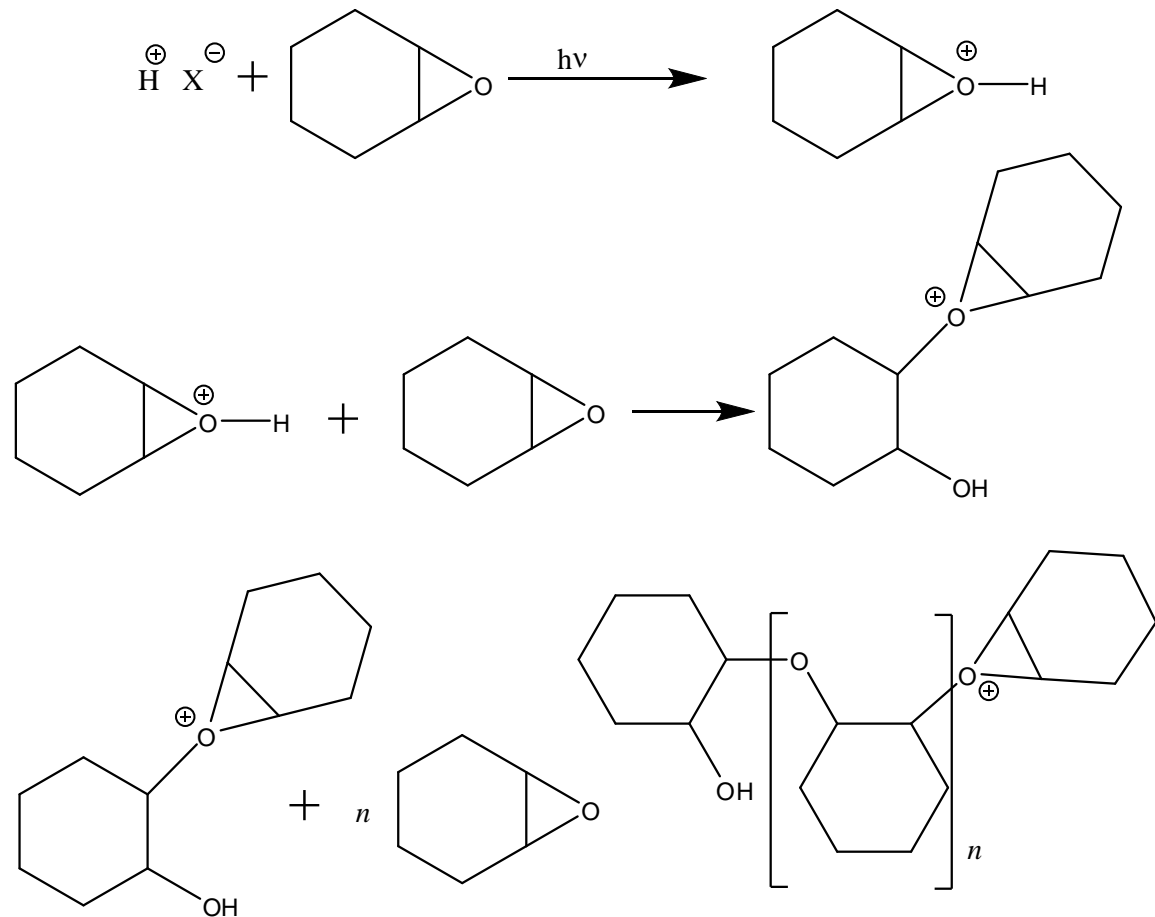


Figure 4.9 The generally accepted mechanism of **CHO** polymerization^[37].

Ring-opening cationic polymerization proceeds in **CHO** in a manner as shown by **Figure 4.9**. Acid protonates the epoxide (which requires a $\text{p}K_{\text{a}}$ of -8 ^[37]). The resulting hydronium salt undergoes nucleophilic attack from an unprotonated monomer. This nucleophilic attack regenerates an onium salt and once again is attacked by another monomer. This process repeats ad infinitum until the monomer expires. Because ring-opening polymerizations are living polymerizations, they can not be stopped^[40].

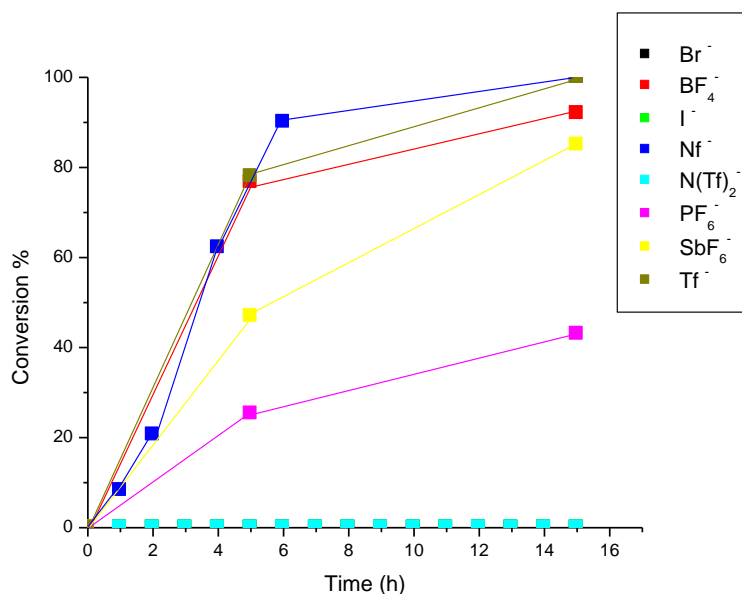


Figure 4.10 Rates of polymerization from 5% (w/w) loading of **NM6HQ** salts with **CHO** in d_6 acetone.

Figure 4.10 lists the results of the cyclohexene oxide ring-opening experiment. **NM6HQ-Nf** clearly showed the fastest polymerization, followed by the **Tf** salt. While **BF₄⁻**, **SbF₆⁻** and **PF₆⁻** were clearly capable of initiating the reaction, they did so at a much slower rate than the fluorinated sulfonyl counterions and were unable to achieve completion over the course of fifteen hours.

It is important to note that several counterions of **NM6HQ** salts were unable to polymerize **CHO**. The **I⁻**, **Br⁻** and **N(Tf)₂⁻** salts did not initiate polymerization, despite exhibiting strong proton transfer to solvent in alcohols, demonstrated in the previous chapter. This suggests that the counterion could be competing strongly for the proton in acetone solvent, yet alcohols are the stronger conjugate bases for the proton than the counterion of the molecule when alcohols are the primary solvent.

It is also important to note that neither of the 6-methoxy- compounds (**NM6MQ-I** and **NM6MQ-Nf**) were capable of initiating polymerization. While **NM6HQ-Nf** shows the fastest rate of polymerization as well as the strongest proton transfer to solvent, the **NM6MQ-Nf** salt is incapable of initiating polymerization. This suggests two conclusions:

- 1.) The 6-methoxyquinolinium compounds are not capable of proton transfer because no proton is attached to the oxygen at the 6-position; proton transfer is definitely coming from the hydroxyl.
- 2.) It is possible to conclude that a latent acid from photochemical degradation of the anion, thereby generating hydrofluoric acid is not occurring; if that was the case, then the **NM6MQ-Nf** would initiate polymerization at roughly the same rate as the 6-hydroxy salt. This salts has been shown to be incapable of initiating polymerization

Dicyclopentadiene Diepoxide

To confirm **NM6HQ-Nf** is in fact capable of cationically photoinitiating epoxides, another monomer, dicyclopentadiene diepoxide (**DCPDE**) was selected. This monomer is a solid, in contrast to **CHO** which is a volatile liquid. This monomer is utilized in the semiconductor industry because of its excellent film-forming capabilities. Photoinitiation of this monomer was carried out in an analogous manner to that of **CHO**; it was also prepared at 5% (w/w) catalyst to monomer loading in acetone. Aside from the new monomer, the experimental preparation is exactly the same method as that described in the previous experimental section.

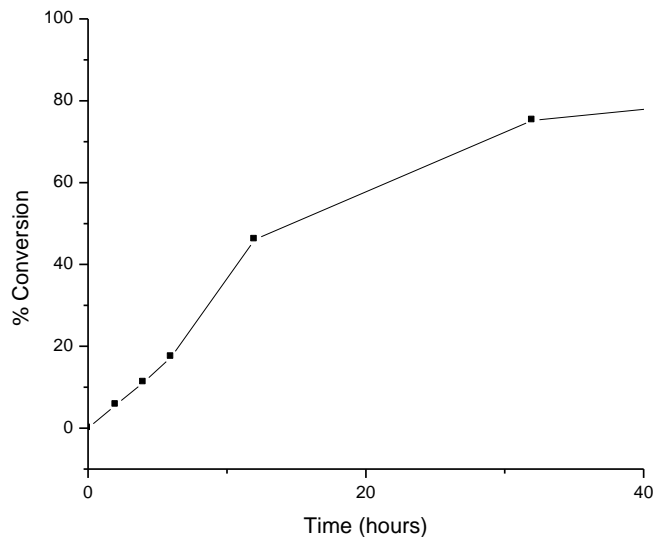


Figure 4.11 Polymerization of **DCPDE** with **NM6HQ-Nf**

Polymerization was successful with **DCPDE** in acetone. The conversion percentage, as determined by NMR can is shown in **Figure 4.11**.

Bisphenol A Diglycidyl Ether

Polymerization was also attempted with bisphenol A diglycidyl ether (**BADGE**). This polymerization attempt was not successful at room temperature with any of the aforementioned **NM6HQ** salts, but it is well known that aliphatic epoxides can not be polymerized without an elevated curing temperature^[39].

Discussion

These experiments lead to several key observations. From these observations, several rules can be outlined:

- 1.) Proton transfer appears to be the driving force behind the polymerizations.

NM6MQ compounds are incapable of initiating polymerization regardless of the counterion, suggesting that initiation is indicative of proton transfer from the hydroxyl.

- 2.) Compounds with strong nucleophiles (**I**, **Br**⁻, **N(Tf)₂**⁻) do not initiate polymerization.

Despite the fact that these stronger conjugate base salts exhibit excellent PTTS in alcohols, a disconnection occurs between photochemical and photoinitiation results. While these strongly nucleophilic salts would be expected to possess competitive polymerization results based on their PTTS spectroscopic studies as a guide, results show that they are incapable of initiating a photopolymerization. A likely reason behind this is competition for the proton between the nucleophilic counterion, the solvent, and the monomer. This competition is very pronounced in acetone, and the counterion may be recombining with the anion before the monomer has the chance to react with it.

- 3.) Bulky non-coordinating counterions (**PF₆**⁻, **SbF₆**⁻, **BF₄**⁻) do not polymerize as effectively as the fluorinated sulfonyl counterions (triflate, nonaflate).

The very weakly-coordinating nucleophiles unexpectedly show both a reduced PTTS and a slower polymerization rate. Although these bulky and uncompetitive counterions are known in traditional onium PAGs to increase the rate of polymerization^[39], they decrease the rate of proton transfer for the **NM6HQ** cation. The exact cause of this is beyond the scope of this thesis, but at

least two reasons for this behavior can be postulated: excited-state electron transfer from the anion to **NM6HQ** which is neutralizing the cation by delocalizing charge throughout the ring structure, thereby allowing the hydroxyl to retain a higher electron density and hindering proton dissociation; or the counterion is disrupting reorganization of the solvent shell surrounding the cation upon excitation, thus inhibiting PTTS and inhibiting the consequent polymerization.

4.) Polymerization only occurs in an inert medium.

Polymerizations are not observed in H₂O, DMSO or methanol. This suggests that strong competition from the solvent for the liberated proton hinders polymerization. Polymerizations have been successful only in acetone with low water content (<0.1% water). Speculation suggests that the polymerization rates would occur even faster in acetonitrile since acetone competes with the monomer for protolysis, demonstrated by **Figure 4.4** and **Figure 4.5**.

5.) Curing times are much longer than industrial PAGs.

Compared to onium salts, which tend to polymerize to near completion within one minute following exposure, polymerization by ESPT takes place on the timescale of hours. Quick curing times are ideal for strong functional materials, however these are formed at the expense of losing sensitivity^[41].

Slower curing materials may shed promise on creating smaller and/or more sharply defined structures at the nanoscale, and may have specialized applications (e.g. UV-active initiators for self-healing polymers).

Despite the success that has been demonstrated utilizing the **NM6HQ** salts in a photoacid-generating capacity, and in verifying that proton transfer is indeed from the hydroxyl group, an unexplained outcome remains. It was anticipated that **NM6HQ** would act as a “true” transient photoacid, reverting to its pre-exposure pH once the photochemical reaction was terminated. However, it appears to irreversibly acidify the acetone solution following exposure.

When the aliquots of the unexposed photoacid (dissolved in acetone) are added to an unbuffered, pH-neutral solution, there is no observable change in pH to two decimal places. Upon photoirradiation, addition of the photoacid to the same neutral solution can drop the pH by as much as one unit. This case is seen equally in methoxyquinoliniums and hydroxyquinoliniums, and the effect was universal across all anions tested. This fact suggests an acid-generating degradation of some sorts, but no degradation products are seen in NMR. Although methoxy- and hydroxyl- quinolinium salts are both somehow generating latent acid, only the hydroxyquinoliniums have initiated an acid catalyzed reaction. No conclusive explanation has been developed yet. This is an area which will require further study.

Conclusions

This chapter has demonstrated the use of **NM6HQ** salts as photo initiators, with proton transfer conclusively coming from the phenolic group.

As photochemical experiments displayed in Chapter 3, the anion plays a significant, albeit not a straightforward role in determining the rate of reaction. In traditional PAG chemistry, the rate of polymerization is dominated by the nucleophilicity of the counterion since the conjugate acid of that anion is formed. Normally, very non-nucleophilic counterions such as SbF_6^- give the fastest rates of polymerization due to their inability to react with a proton. This is clearly not the case with photochemical reactions initiated by ESPT. The rates of polymerization tend to mirror the efficiency of proton transfer as determined by steady state fluorescence spectroscopy, although strong nucleophilic counterions compete with the monomer for the proton in inert solvents, thereby rendering them unable to initiate polymerization.

The Förster cycle predicts an excited-state photoacidity of $\text{p}K_a \sim -7$ for **NM6HQ**, based upon the large bathochromic shift between the cation and the zwitterion. Proton exchange with acetone reaffirms an excited state photoacidity of at least -7 . However the cationic ring opening of **CHO** requires a $\text{p}K_a < -8$ ^[37], suggesting that several **NM6HQ** salts examined are more potent than the Förster cycle predicts. In summary, **NM6HQ** salts are acting as long-wavelength photoinitiators through ESPT rather than through solvent hydrogen abstraction.

CHAPTER 5

NM6HQ FRONTIERS

Though the aims of this thesis are to demonstrate salts of the **NM6HQ** family as extremely powerful excited-state proton donors, the applications for transient acid generation from hydroxyquinoliniums are only limited to the imagination and too numerous to be listed in this text.

Two immediate applications conceived through experimentation should be mentioned as potential future applications of **NM6HQ** salts.

NM6HQ-N(Tf)₂ A Room Temperature Ionic Liquid capable of ESPT

The field of ionic liquids has grown by leaps and bounds in recent years, as industry and academia look for practical solutions in “green chemistry”.

As their name infers, ionic liquids are liquids which are composed entirely of ions, and often comprise quaternary ammonium compounds (i.e. imidazolium and pyridinium) in conjunction with weakly-coordinating conjugate bases^[42]. Reactions performed in room temperature ionic liquids (RTILs) are often desirable; reactions such as Friedl-Crafts alkylation^[43] and Diels-Alder cycloadditions^[44] have been successfully developed. Likewise, ionic can possess favorable qualities for separating products and starting materials. Due to the low vapor pressure of these solvents, they are viewed as environmentally friendly and less hazardous to work with compared to volatile and explosive solvents^[45].

NM6HQ-N(Tf)₂ was found to have an abnormally low melting point (18-22 °C) after thorough desiccation compared to the other **NM6HQ** salts synthesized. It is a viscous liquid at room temperature. Although it exhibits strong proton transfer in alcohols, the compound is incapable of proton transfer to an epoxide. Despite this fact, it is conceivable to use this as a photoactive RTIL for proton transfer reactions requiring a slight pK_a jump to initiate the reaction. A RTIL of this type would also signify one of the first literature reports of quinolinium ionic liquids^[46].

Ratiometric Fluorescence Sensing

“Turn-on” fluorescence sensors are more desirable than fluorescence sensors based on fluorescence quenching, and have greater application. **Figure 5.1** shows that **NM6HQ** could act as a sensor in mixed aqueous media. The fluorescence quantum yield of **Z*** at 490 nm in a proton-accepting solvent such as DMSO shown here is negligible. However, the fluorescence quantum yield increases by a factor of over 1000 when proton transfer is inhibited by solvent, in this case acetonitrile, allowing for emission from **C***. This property could be useful for detection of small quantities of proton acceptors, for instance, determining the water content in a solvent or in a portion of a living cell. While this capacity of **NM6HQ** has not been fully explored, a similar literature citation utilizes 1-naphthol to sense the water content of a polymeric alcohol hydration^[47].

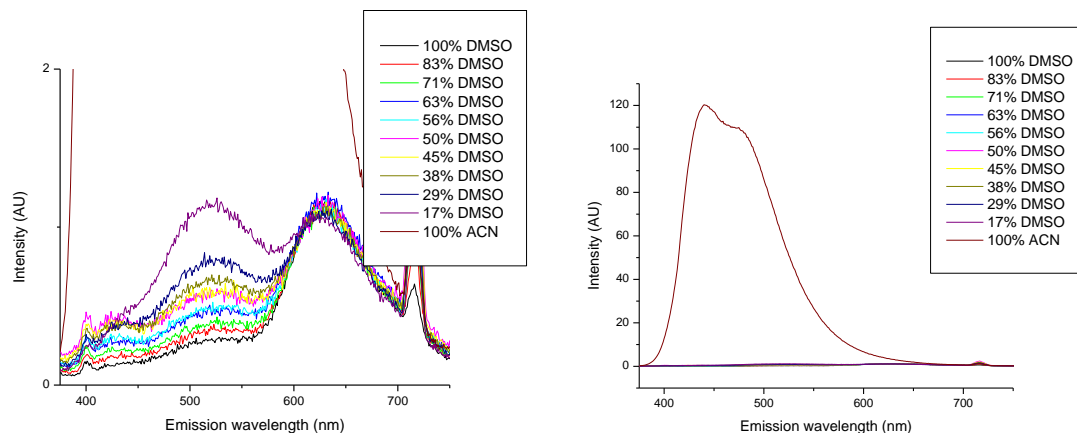


Figure 5.1 Behavior in proton accepting and non-accepting environments.

Final Thoughts

This thesis has aimed to demonstrate the powerful potential of *N*-methyl-6-hydroxyquinoline as a powerful proton donor upon excitation. The studies in this thesis have attempted to lay the groundwork for even more powerful molecules exhibiting excited-state proton transfer from hydroxyarenes in future studies. Although the counterion effects have not yet been fully reconciled, they apparently play a large role in determining proton transfer to solvent and in the initiation of photochemical reactions.

NM6HQ has exhibited the largest pK_a jump to date as evidenced by its spectroscopic properties, and several of the compounds investigated are the first to initiate photochemical reactions by proton transfer and to demonstrate that the hydroxyl proton is the proton responsible for the photoinitiation of cationic polymerizations.

The applications of ESPT are numerous, and two examples that have tremendous potential, yet are neither fully appreciated nor extensively investigated in the chemical literature have been mentioned.

REFERENCES

1. BBC, *History of Chemistry - Acids and Bases*. 2008.
2. Oxtoby, D.W., W.A. Freeman, and T.F. Block, *Chemistry: Science of Change*. Fourth Edition 2003.
3. Fischer, E., USPTO Patent # 3,236,784. 1966, Farbwerke Hoechst AG.
4. Weber, K., *Z. Phys. Chem*, 1931. **B15**(18).
5. Terenin, A.N. and A. Kariakin, *Nature*, 1947. **159**: p. 881-882.
6. Förster, *Naturwiss*, 1949. **36**(186).
7. Ireland, J.F. and P.A.H. Wyatt, *Adv. Phys. Org. Chem*, 1976. **12**(131).
8. Arnaut, L.G. and S.J. Formosinho, *J. Photochem. Photobiol. A*, 1993. **71**(1).
9. Tolbert, L.M. and K.M. Solntsev, *Acc. Chem. Res.*, 2002. **35**: p. 19-27.
10. Crivello, J.V. and K. Dietliker, *Photoinitiators for Free Radical, Cationic and Anionic Photopolymerization*. 1998.
11. Hino, T. and T. Endo, *Macromolecules*, 2004. **37**(5): p. 1671-1673.
12. Sato, S.L., Donna L.; Raleigh, Daniel P, *Biochemistry*, 2000. **39**(16).
13. Kaczmarek, L., P. Borowicz, and A. Grabowska, *J. Photochem. Photobiol. A*, 2001. **138**(2).
14. Rudawsky, A.C. and S.J. Schmidtke, *Abstracts of Papers, 235th ACS National Meeting*, 2008.
15. Tolbert, L.M. and J.E. Haubrich, *Journal of the American Chemical Society*, 1994. **116**(23).
16. Nunes, R.M.D., et al., *J. Am. Chem. Soc.*, 2005. **127**(34).
17. Genosar, L., et al., *Journal of Physical Chemistry A*, 2005. **109**(21).
18. Tolbert, L.M. and J.E. Haubrich, *J. Am. Chem. Soc.*, 1990. **112**(22).

19. Soroka, K., et al., *Anal. Chem.*, 1987. **59**(629).
20. Bardez, E., et al., *J. Phys. Chem.*, 1994. **98**(9).
21. Solntsev, K.M., et al., *J. Am. Chem. Soc.*, 2005. **127**(23).
22. Kim, T.G. and M.R. Topp, *J. Phys. Chem. A.*, 2004. **108**(46).
23. Perez-Lustres, J.L., et al., *J. Am. Chem. Soc.*, 2007. **129**(17).
24. Van den Berg, O., W.F. Jager, and S.J. Picken, *J. Org. Chem.*, 2006. **71**(7).
25. Van den Berg, O., et al., *Macromolecules*, 2006. **39**(1).
26. Koppel, I., *J. Am. Chem. Soc.*, 2000. **122**: p. 5114-5124.
27. Arnett, E.M. and J.N. Anderson, *J. Am. Chem. Soc.*, 1963. **85**: p. 1542-1543.
28. Anslyn, E.V. and D.A. Dougherty, *Modern Physical Organic Chemistry*. 2006.
29. Clower, C., et al., *J. Phys. Chem. A.*, 2002. **106**(13).
30. Crivello, J.V. and J.H.W. Lam, *Polym. Sci. Polym. Chem. Ed.*, 1980. **18**.
31. Jarnagin, N.D., et al., *Proceedings of SPIE-The International Society for Optical Engineering*, 2006. **Pt. 2, Advances in Resist Technology and Processing XXIII**.
32. Harada, Y., T. Yoshida, and Y. Takada, *Faming Zhuanli Shenqing Gongkai Shuomingshu*, 2008.
33. Shimomura, O., I. Tomita, and T. Endo, *Journal of Polymer Science, Part A: Polymer Chemistry*, 2001. **39**(6).
34. Houlihan, F.M., et al., *Photoresist composition for deep UV and process thereof*, USPTO 2006.
35. Rahman, M.D., et al., *Novel photoactive sulfonium compounds as photoacid generators for positive photoresist compositions*, USPTO. 2005.
36. Seiler, P. and J. Wirz, *Tetrahedron Lett.*, 1971: p. 1683-1686.
37. Soucek, M.D. and J. Chen, *Journal of Coatings Technology*, 2003. **75**.

38. Crivello, J.V. and M. Sangermano, *Visible and Long-Wavelength Cationic Photopolymerization*, in *Photoinitiated Polymerization*. 2003.
39. Crivello, J.V., *Photoinitiators for Free Radical Cationic and Anionic Photopolymerization*. 1998, New York: Wiley.
40. Zhang, Y., et al., *Designed Monomers and Polymers*, 2005. **8**(6): p. 571-588.
41. Crivello, J.V., *Photoinitiated Polymerization*. 2003, Washington, DC: American Chemical Society.
42. Swatloski, R.P., J.D. Holbrey, and R.D. Rogers, *Green Chem.*, 2003. **5**: p. 361-363.
43. Valkenberg, M.H., C. deCastro, and W.F. Hölderich, *Applied Catalysis A: General*, 2001. **215**(1-2): p. 185-190.
44. Fischer, T., et al., *Tetrahedron Lett.* **40**(4): p. 793-796.
45. Huddleston, J.G., et al., *Green Chem.*, 2001. **3**: p. 156-164.
46. Kazheva, O.N., et al., *Zhurnal Neorganicheskoi Khimii*, 2007. **52**(4): p. 620-624.
47. Kumar, A.C. and A.K. Mishra, *Talanta*, 2007. **71**(5): p. 2003-2006.